Effect of polarity of solvent on silanization of halloysite nanoclay using (3-Glycidyloxy propyl) trimethoxy silane

A.M. Abu El-Soad[a, b**], G. Lazzara [c*], A. V. Pestov [a, d], G. Cavallaro [c], N. A. Martemyanov [a] , E.G. Kovaleva[a].

[a]Ural Federal University, Mira St. 19, Yekaterinburg 620002, Russia
[b] Nuclear Materials Authority, P.O. Box 530, El Maadi, Cairo, Egypt
[c] Dipartimento di Fisica e Chimica, Università degli Studi di Palermo, Viale delle Scienze, Parco d'Orleans II, Ed. 17, 90128 Palermo, Italy
[d]Institute of Organic Synthesis, Ural Branch of the Russian Academy of sciences, Yekaterinburg, Russia.

Corresponding authors:
*** Giuseppe Lazzara** (giuseppe.lazzara@unipa.it**)** Università degli Studi di Palermo, Viale delle Scienze, Parco d'Orleans II, Ed. 17, 90128 Palermo, Italy

****A.M. Abu El-Soad** (chemistasmaa60@yahoo.com) Ural Federal University, Mira St. 19, Yekaterinburg 620002, Russia

Abstract

The grafting of silane groups on clay surfaces has been recently investigated in order to fabricate versatile compounds with new potential applications in materials science and ecological engineering. This work inspected the influence of variety of solvents on the silanization of halloysite nanoclay (HNC) surface by (3-Glycidyloxy propyl) trimethoxy silane. Functionalization of halloysite nanoclay (HNC) by 3-Glycidyloxypropyltrimethoxysilane (GOPTMS) has been performed in polar protic solvents (Ethanol), polar aprotic solvents (Tetrahydrofuran (THF) and Acetonitrile) and non-polar solvents (Hexane, 1,4-Dioxane and Toluene) as dispersing media. The silane grafted materials were distinguished by using Fourier Transform Infrared Spectroscopy (FT-IR), elemental analysis, Scanning Electron Microscopy (SEM), Thermogravimetry (TGA), X-ray Diffraction Analysis (XRD) and Nitrogen adsorption/desorption isotherms. The greatest percent of the loaded silane was obtained by using Hexane as a solvent.

Keywords: Halloysite, solvent, solubility parameters, thermogravimetric analysis, FT-IR, XRD.

1. Introduction

In recent years, clay nanoparticles have been of great attention owing to their suitability in various technological fields, such as remediation, materials science, drug delivery and ecological engineering [1–6]. Due to the demand of these applications, surface modification of clay minerals has been manipulated in order to improve their properties. The surface of clay minerals can be modified using physical and chemical modes. The physical mode which is mightily utilized for modifying clay mineral surface, is that uses surfactants and provides preparation of inorganic/organic hybrid materials[7,8]. Clays can be chemically adjusted by using exchangeable cations and organics. These modes of amendment inspire changing for many parameters such as surface properties (sizes, specific surface, porosity and charge) as well as cation exchange and absorption abilities for wider implementations [9]. Halloysite ($Al_2(OH)_4Si_2O_5.\ nH_2O$) is an example of nanosized clay minerals which is linked to the kaolin class [10,11]. It is naturally occurring mineral, having a hollow tubular structure[12–14]. It is a biocompatible nanoclay that possesses a lumen and an external diameter of 100–150 Å and 500–800 Å, respectively, and it is composed by one octahedral sheet of alumina and one tetrahedral sheet of silica [15–18]. The inner and outer surfaces of halloysite have diverse chemical installation and displays a net negative zeta potential in a pH from 2.5 to 8.5 because of the rolling of these sheets. The positive charge appears on the octahedral alumina sheet while the negative charge appears on the tetrahedral sheet of silica and this negative charge dominates the net charge of the nanotubes[19,20]. Taking this into consideration, the outer surface of halloysite nanotubes have hydroxyl groups which are covalently reacted with organic reagents like organosilane and organophosphonic acid etc.[21]. This may modify the physicochemical property of halloysite by altering the charge of the surface from a negative to a positive charge [22]. Organosilanes are mightily used for amendment of halloysite nanotubes surface because they cause reduction in hydrophobicity by making the surface hydrophobic owing to a diminutive number of Si–OH groups [23,24]. kaolinite has been amended using (3-glycidyloxypropyl) trimethoxy silane and tetraethyl orthosilicate (TEOS) as reported by Zhang et al. (2012) because the loaded silane decreased the hydrophilicity of the kaolinite particles and amended the compatibility with the rubber mold [25,26]. Silylation of halloysite nanotubes

surfaces is very sensitive to the nature of dispersing media used, so many solvents with diverse polarity and diverse dielectric constant have been used in this work. In the present work, (3-Glycidyloxy propyl) trimethoxy silane has been chemically grafted on HNC surface using variety of solvents. The new insights obtained in this work are of great significance for comparing the efficiency of several solvents on chemical grafting and developing an efficient silylation technology. The grafted products have been distinguished by using various techniques such as Fourier Transform Infrared Spectroscopy (FT-IR), Scanning Electron Microscopy (SEM), Thermogravimetry (TGA), X-ray Diffraction Analysis (XRD), Nitrogen adsorption/desorption models and elemental analysis.

2. Experimental section

2.1. Materials and reagents

Halloysite nanoclay (HNC) was provided by Sigma-Aldrich. The trifunctional organosilane agent (3-Glycidyloxy propyl) trimethoxy silane [GOPTMS] was purchased from Alfa Aesar, China. Toluene, Ethanol, Tetrahydrofuran (THF), Acetonitrile, n-Hexane and 1,4-Dioxane were of analytical pureness. The other reagents were obtained from local companies in Russia and they are of analytical grade and were used without any treatment.

2.2. Chemical grafting of GOPTMS on HNC surface

In a dry flat bottom boiling flask add 1.3 g of HNC then add 10 ml of solvent and were kept in contact for 30 min. under agitation conditions to obtain good dispersion state then insert into the reaction media 6.3 mmoles of (3-Glycidyloxy propyl) trimethoxy silane and agitated for additional 30 min. at room temperature then refluxed for 2 hours. Polar protic solvents (Ethanol), polar aprotic solvents (Tetrahydrofuran (THF) and Acetonitrile) and non-polar solvents (1,4-Dioxane, Toluene and n-Hexane) were tested in these experiments. The grafted HNC samples were discrete by filtration, rinsed several times with 50 ml of acetone then, dehydrated in an oven for 6 hours at 78 °C. Figure 1 displays the sketch for chemical grafting of GOPTMS on HNC surface.

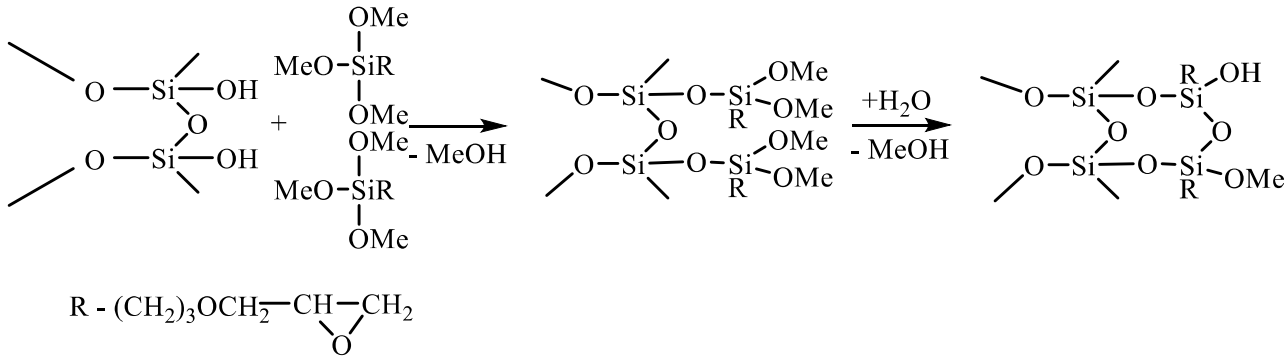

Fig. 1. The sketch for chemical grafting of GOPTMS on HNC surface.

2.3. Characterization

The content (%) of C, H and N of the grafted HNC samples was provided by Elemental analysis. The analysis was accomplished by Perkin Elmer PE 2400 analyser. The grade of grafting of GOPTMS on HNC surface was evaluated by Eq. (1):

$$Grade\ of\ grafting = \frac{\%\ of\ carbon\ obtained\ from\ EA}{theoretical\ \%\ of\ carbon\ content} \quad (1)$$

Where the theoretical % of carbon content equal 19.6% by using the equation reported in our previous work [27].

Fourier transform infrared spectra was acquired by a spectrum-one spectrometer, Perkin Elmer analyser. The measurements were performed with a wave number varied between 4500 and 500 cm^{-1}. Thermogravimetry was conducted by a Metler Tolledo instrument in order to explore the thermal response of the grafted HNC samples. In the range of temperature changes from 30°C to 1000°C and the heating ramp is 20°C/min, the mass of the sample was measured as function of time under a nitrogen flow of 60 ml/min. Calibration has been done using the procedure reported by Blanco et al. (2017) [28,29]. Weight % loading of organic moiety on the surface of HNC can be estimated by Eq. (2)[30]:

$$Silane\ loaded\ \ (Wt.\%) = 100\ [1 - \frac{MR_{\ 600\ composite} + ML_{150\ composite}}{MR_{600\ pristine} + ML_{150\ pristine}}] \quad (2)$$

where $MR_{600\ composite}$ and $MR_{600\ pristine}$ is the residual matter at 600 °C for functionalized HNC and pristine HNC samples, respectively. $ML_{150\ composite}$ and $ML_{150\ pristine}$ represent the mass losses in the temperature interval 25-150 °C for the functionalized HNC and pristine HNC samples, respectively.

The morphological features of pristine HNC and the sample with the greatest organic content was evaluated by SEM images which were gained by using a Carl Zeiss EVO LS 10 device. X-ray diffraction (XRD) (XPERT PRO MPD analytical diffractometer) was used to identify the crystalline phases in both pristine and grafted halloysite nanoclay samples. The diffractograms were recorded in the angle range (2θ) of 7–31°. The 2θ step size and a counting time were set at 0.01° and 2.0 step/s, respectively [31].

Adsorption/desorption isotherms for Nitrogen were estimated at controlled temperature (-196 °C) by a Micrometrics Gemini VII 2390 instrument. The functionalized HNC products and pristine HNC have been degassed for 3 hours in the presence of vacuum at 120°C before adsorption experiments. Brunauer-Emmett-Teller (BET) and Barrett-Joyner-Halenda (BJH) models were used to calculate the specific surface area, pore size distributions and the pore volume.

3. Results and discussion

3.1. Elemental analysis characterization:

Table 1 shows the data acquired from elemental analysis of C, H and N contents for the grafted HNC samples. It appears that the greatest grade of the grafting process has been gained by the sample grafted with (3-glycidyloxypropyl) trimethoxy silane in the presence of n- Hexane as a dispersing media. This indicated that the solvent with low value of Dielectric constant is more appropriate for the grafting process.

Table 1. Elemental analysis of HNC samples which have been chemically grafted in various types of solvent using the trifunctional organosilane agent [GOPTMS].

Sample	Content, %			Solvent	Degree of functionalization %
	C	H	N		
SZ1	8.98	2.73	0.00	Toluene	45.6
SZ2	8.56	2.66	0.00	THF	43.5
SZ3	4.56	2.19	0.00	Ethanol	23.2
SZ4	18.31	3.9	0.00	n-Hexane	93.3
SZ5	4.12	2.15	0.00	1, 4 dioxane	21.0
SZ6	4.12	2.12	0.00	Acetonitrile	21.0

3.2. Fourier transform infrared characterization:

Fourier transform infrared spectra of pristine HNC and grafted HNC with (3-glycidyloxypropyl) trimethoxy silane in the presence of several types of solvents are shown in Figure 2. Compared to pristine halloysite, some new signals were lighted for the sample (SZ4) which has been done in the presence of n- Hexane as a solvent. These peaks were noticed at 2930 cm^{-1}, 2860 cm^{-1}, 1725 cm^{-1} and 1200 cm^{-1}. The bands at 2930 cm^{-1} and 2860 cm^{-1} clarify symmetric stretching vibration and asymmetric stretching vibration of CH_2 groups respectively[32]. The asymmetric deformation vibration of CH_2 groups results in a weak band near 1725 cm^{-1}[33]. The deformation vibration of Si-CH_2-R that appears at 1175-1250 cm^{-1} was noticed by the weak band which occurs at 1200 cm^{-1} [34]. These peaks which were clarified for the sample (SZ4) indicate the formation of a cross-linked structure which results from the condensation of OH groups on halloysite nanoclay surface and methoxy groups of GOPTMS. The FT-IR results agree with the elemental analysis data showing that n-Hexane endows the most efficient silanization process.

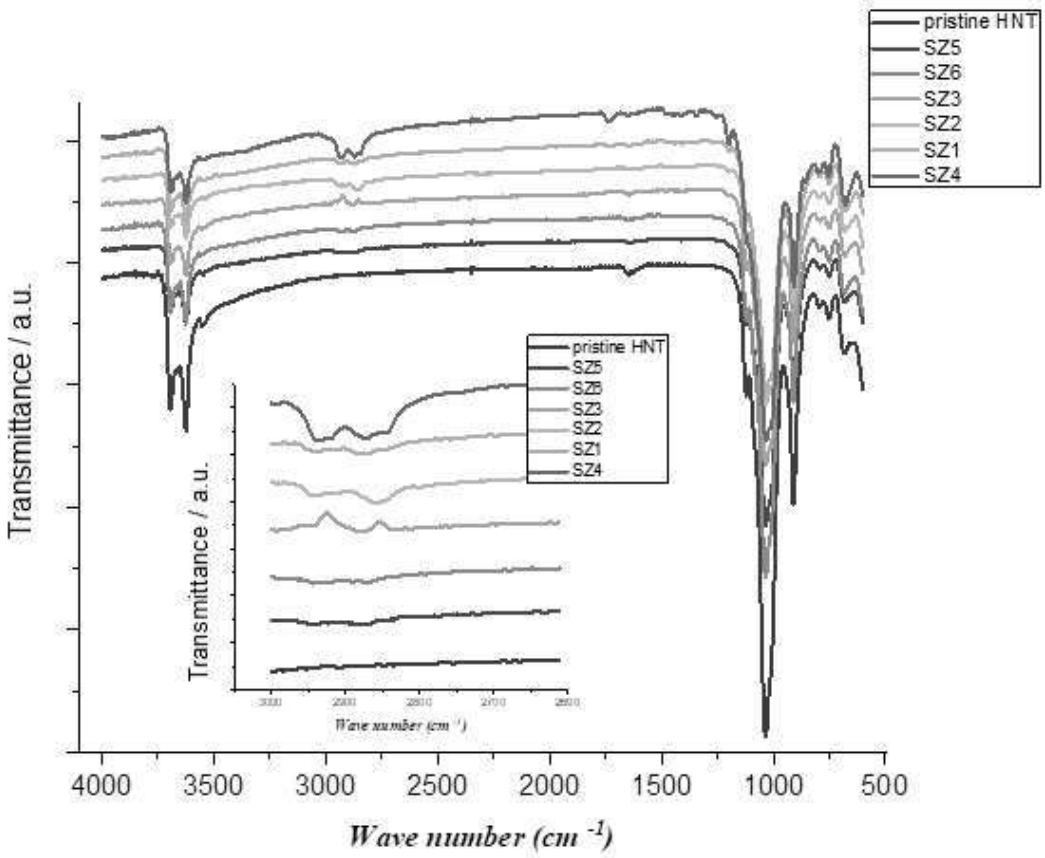

Fig. 2. FT-IR spectra for pristine HNC and HNC samples which are grafted by GOPTMS in the presence of several types of solvents.

3.3. Thermogravimetric analysis (TGA):

Differential thermogravimetric (DTG) and thermogravimetric (TGA) curves of pristine HNC and grafted HNC samples are shown in Figures 3 and 4. The mass loss for pristine HNC below 200°C can be attributed to the water molecules physically linked to the clay interface [35]. It was clarified that the highest mass loss of pristine HNC happened when the temperature verified from 400 to 550 °C and this is imputed to the dehydroxylation of OH groups of HNC [33]. For samples that were prepared in 1,4- Dioxane, Acetonitrile and Ethanol, it was spotted that the highest mass loss in the temperature range from 300 to 500 °C while for the samples that were prepared in n- Hexane, Toluene and Tetrahydrofuran, it was noticed that the greatest mass loss appeared with a wider variation of temperature from (200 to 500 °C). This may be imputed to the silanes physiosorbed on the HNC surface, covalently bonded as a consequence of the condensation reaction that takes place between the hydrolyzed silanes and the HNC hydroxyl groups [36–38]. Table 2

shows the values of the amount of the loaded silane on HNC surface, which was calculated by using Eq. 2. The silane loadings were 23.80 and 12.57 wt% for the grafted samples prepared in n- Hexane and Toluene, respectively. The grafting efficiency was very low using Ethanol as a dispersing solvent. This may be correlated to the fact that polar-protic solvents have the ability to solvate the silanol groups and consequently, a larger amount of GOPTMS is deposited on halloysite surface by oligomerization. This decrease the reactivity of silane molecules towards halloysite nanoclay surface. In case of non-polar solvents, oligomerization greatly restrained, and hence the reaction proceed through the direct condensation of hydrolyzed GOPTMS and the HNC hydroxyl groups (located at the internal wall, at the edge, and at defects of the external surface) as a result of increasing the reactivity of silane molecules towards HNC surface [39,40]. Another important fact that must be considered is the effect of dielectric constant of the solvent that was used as a dispersing media. The solvents that have great values of dielectric constant, having high strength of H-bonding. The H-bonding between GOPTMS and the OH groups will dominate in this case rather than the condensation reaction [41]. For these reasons, n- Hexane was probably the solvent providing the greatest organic content in the composite after the grafting process. To provide a predictive and semiquantitative view on the solvent polarity effect on the loading efficacy, we thought interesting to consider the Hildebrand solubility parameter [42] that are provided in Table 2 for all the investigated solvents. Figure 5 shows that there is a correlation between the solubility parameters of the solvent and Wt. (%) of silane loaded. As the value of the solubility parameters (δ / $J^{1/2}$ $cm^{-3/2}$) increases the value of Wt. (%) of silane loaded decreases to a plateau. Interestingly a threshold limit at ca. 20 $J^{1/2}$ $cm^{-3/2}$ was observed.

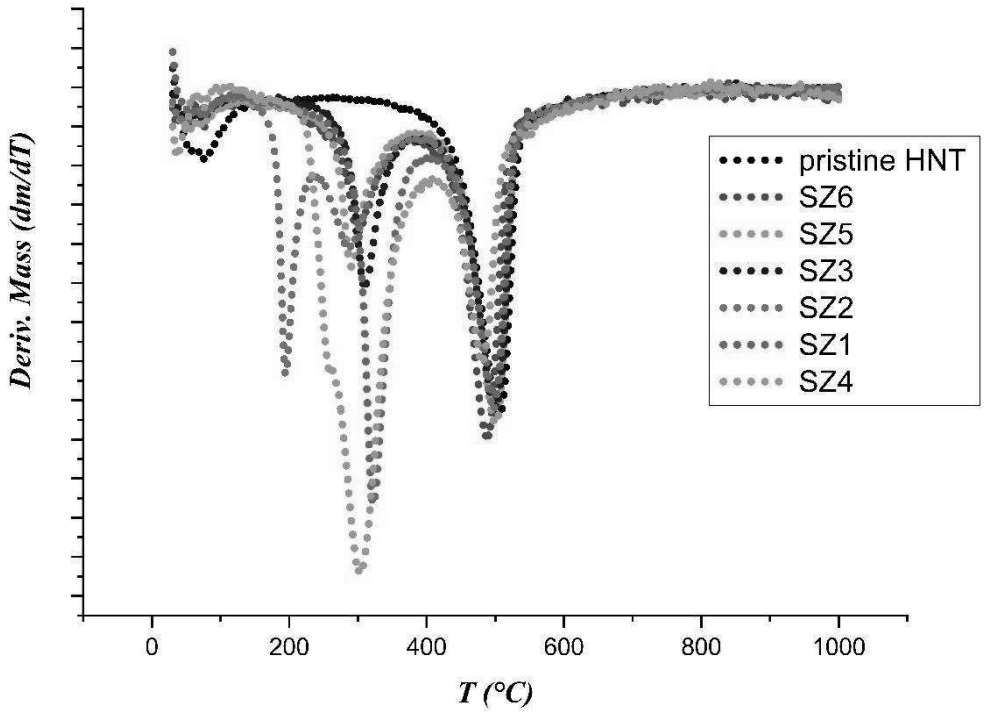

Fig. 3. DTG curves of pristine HNC and grafted HNC samples in the presence of several dispersing media.

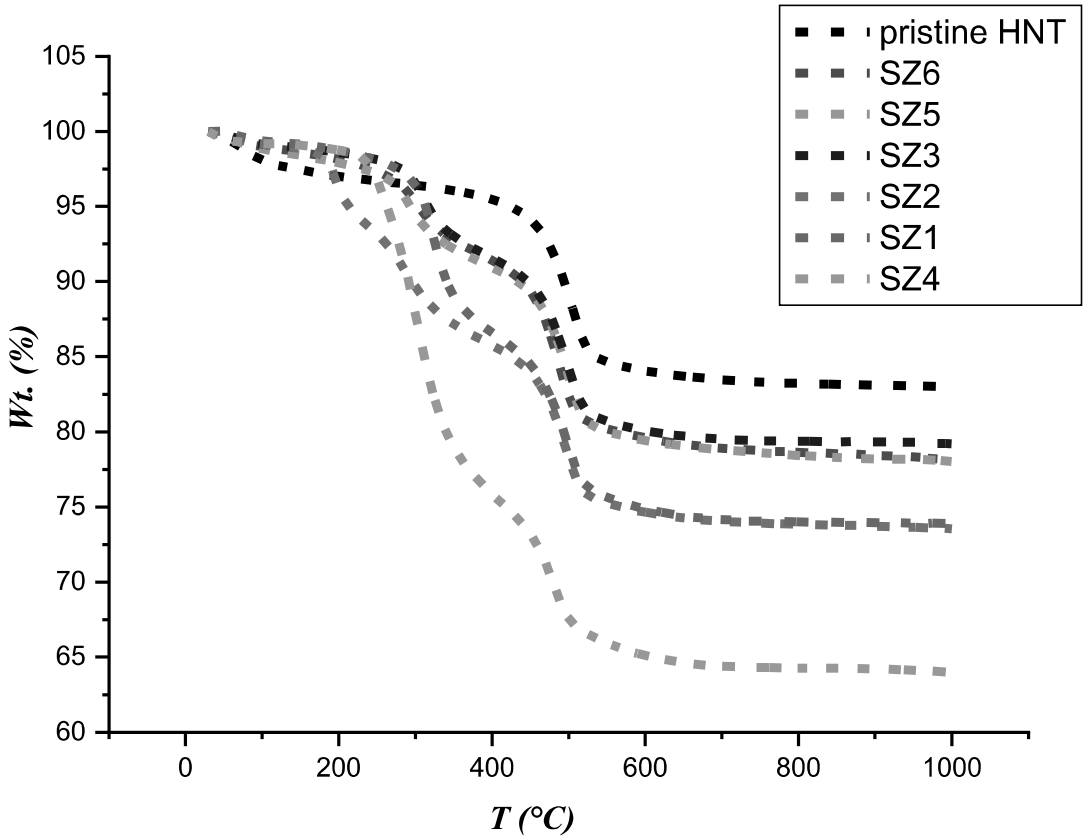

Fig. 4. Thermogravimetric analysis of pristine HNC and grafted HNC samples in the presence of several dispersing media.

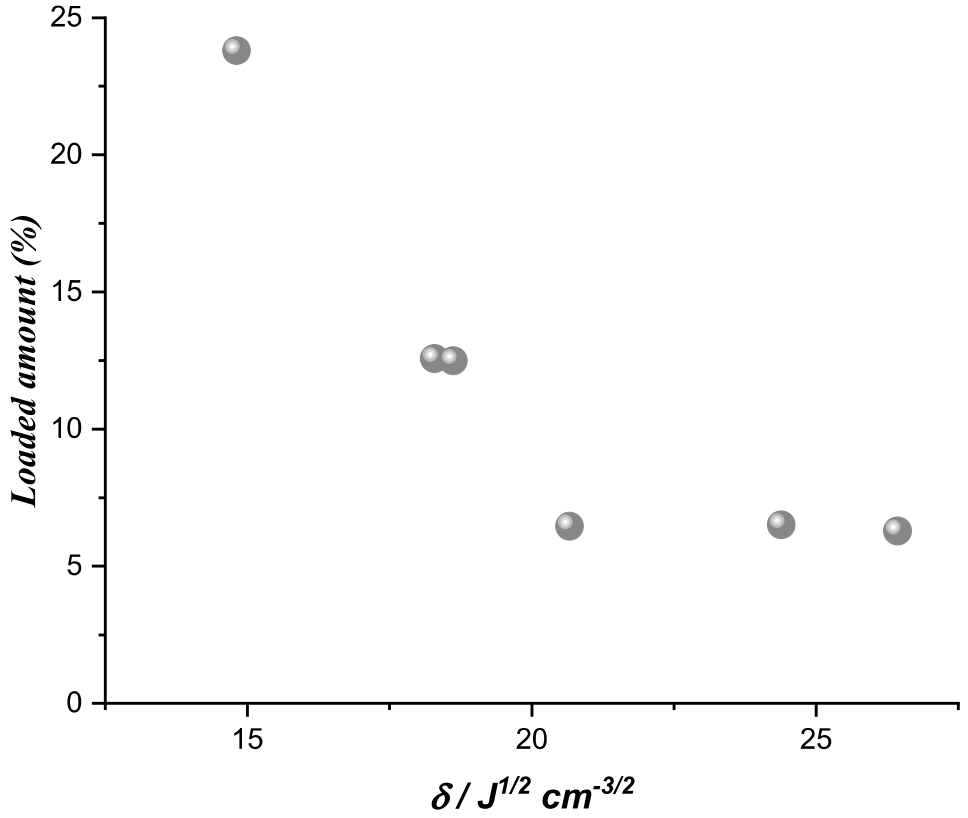

Fig. 5. The relation between Wt. (%) of silane loaded and the solubility parameters.

Table 2. Thermogravimetric analysis of HNC samples which have been grafted in several types of solvent using (3-glycidyloxypropyl) trimethoxy silane.

Sample	Solvent	Dielectric constant	δ / $J^{1/2}$ $cm^{-3/2}$	Loaded amount (%) [a]
SZ1	Toluene	2.4	18.29	12.57
SZ2	THF	7.5	18.62	12.49
SZ3	Ethanol	24.5	26.43	6.28
SZ4	n-Hexane	2.0	14.81	23.80
SZ5	1, 4 dioxane	2.3	20.66	6.46
SZ6	Acetonitrile	37.5	24.39	6.51

[a] Determined by using Eq. (2)

3.4. XRD and SEM analysis

The samples that were functionalized with (3-glycidyloxypropyl) trimethoxy silane in the presence of various solvents were distinguished by using X-ray diffraction

analysis. Figure 6 shows a slight change in the basal spacing in grafted halloysite nanoclay from 7.5 Å (pristine HNC) to ca. 7.4 Å (grafted in Ethanol) or to ca. 7.4 Å (grafted in n-Hexane). This gives an evidence that the GOPTMS intercalation into HNC interlayers does not occur, and the solvent polarity does not significantly affect the interlayer structure of the grafted samples. SEM images were collected for the sample with the greatest organic content (SZ4 in n-Hexane) and compared to pristine halloysite as shown in (Fig.7). In agreement with the high loading of organic moieties determined by TGA, the sample SZ4 shows a SEM image much different than pristine HNC evidencing a composite like morphology where HNC are embedded in an organic matrix.

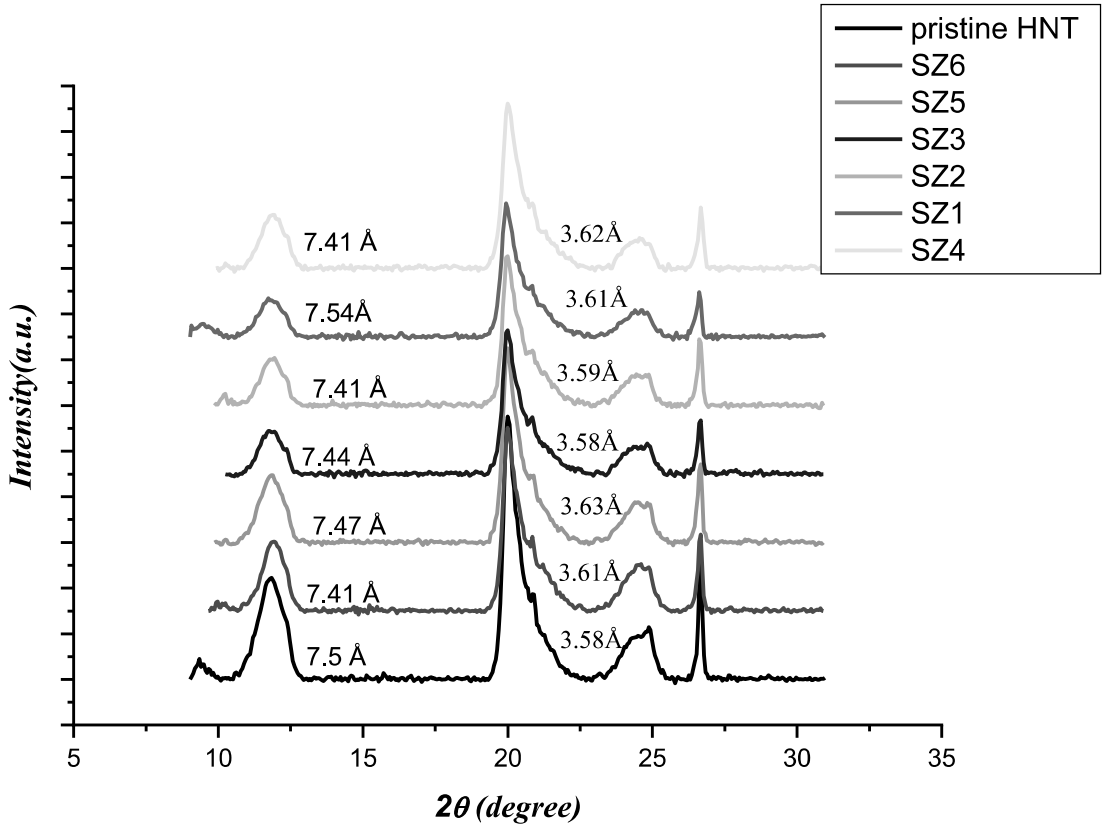

Fig. 6. XRD patterns of pristine HNC and grafted HNC samples in the presence of several dispersing media.

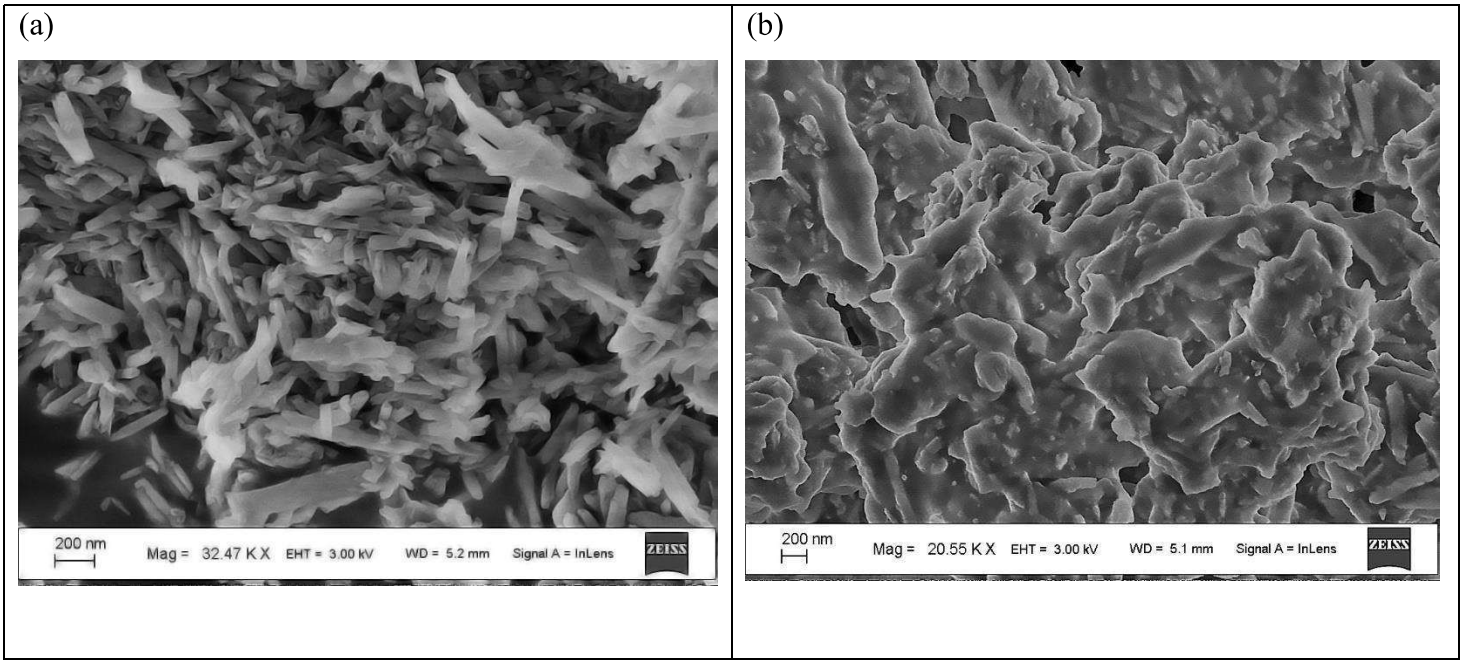

Fig. 7. SEM images for pristine HNC (a) and SZ4 sample (b)

3.5. BET analysis

The Nitrogen adsorption/desorption isotherms and the corresponding pore size distributions are presented in Figure 8 (a, b). The specific surface area has been specified by Brunauer–Emmett–Teller module depending on adsorption/desorption results with variation of the partial pressure (P/P_o) from 0.01 to 0.99, and the total pore volume has been estimated by the quantity of nitrogen adsorbed at a partial pressure of 0.98. Fig. 8 (a) showed that the quantity of N_2 adsorbed displays hysteresis and the N_2 adsorption quantity was rapidly enhanced at a relative partial pressure $\geq$ 0.8. According to IUPAC classification, all the samples show a type II isotherm [43], which is a typical of mesoporous structure. The hysteresis loop of these samples is like type H3, which is typical of agglomerates of plate-like particles containing slit-shaped pores [44]. Table 3 reports the BET surface area, BJH pore volume and the average pore diameter of HNC based samples obtained in different solvents. It is observed that the greatest surface area (m^2/g) acquired for the sample SZ3 which is accomplished in the presence of Polar protic solvent (Ethanol) and with low value of pore diameter (9.1 nm). The highest values of the pore diameter obtained by the samples SZ1 and SZ4 which were prepared in the presence of non-polar solvents. The BET surface changes following a reduction trend with the increase of the loading amount as reported in Figure 9.

(a)

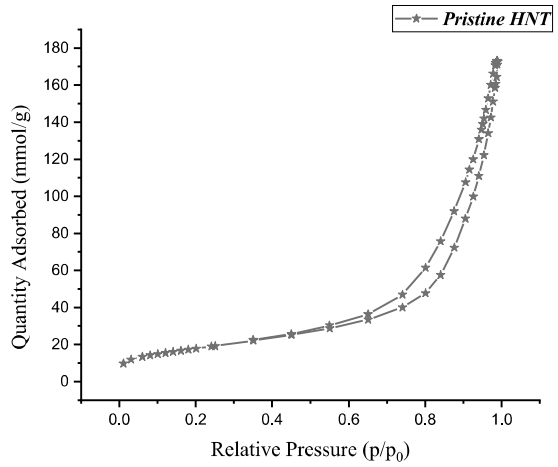
Pristine HNT
Quantity Adsorbed (mmol/g)
Relative Pressure (p/p0)

(b)

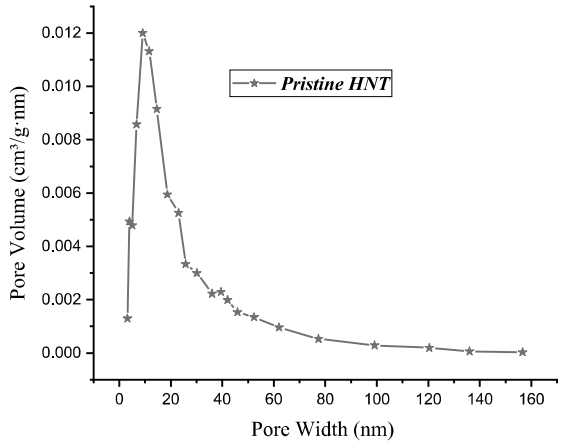
Pristine HNT
Pore Volume (cm3/g·nm)
Pore Width (nm)

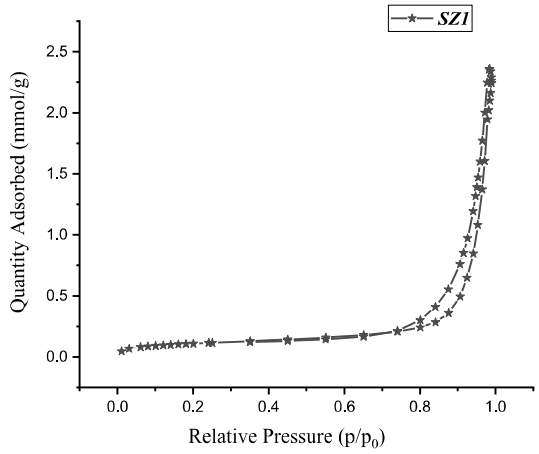
SZ1
Quantity Adsorbed (mmol/g)
Relative Pressure (p/p0)

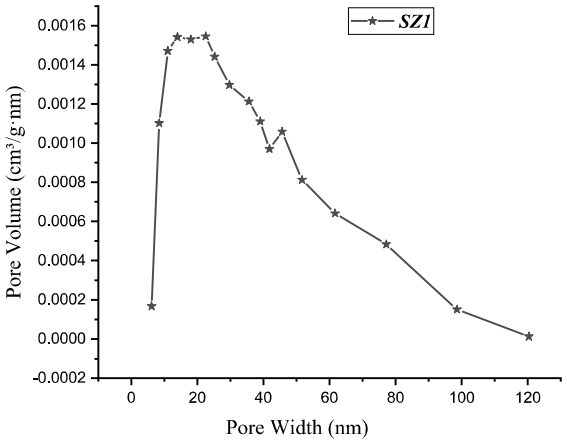
SZ1
Pore Volume (cm3/g·nm)
Pore Width (nm)

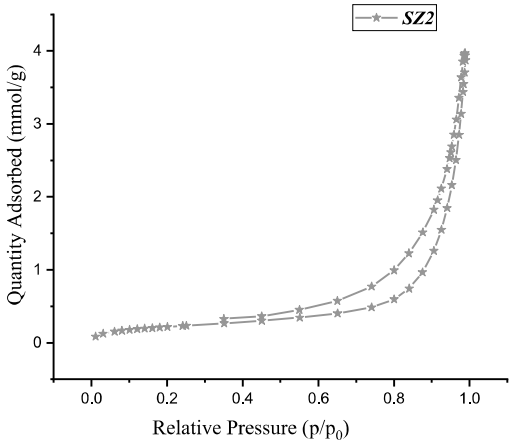
SZ2
Quantity Adsorbed (mmol/g)
Relative Pressure (p/p0)

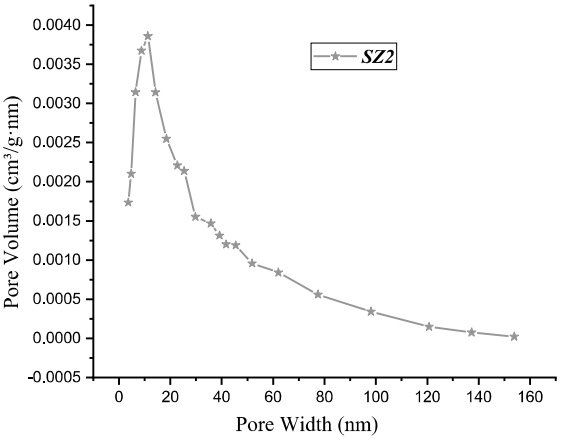
SZ2
Pore Volume (cm3/g·nm)
Pore Width (nm)

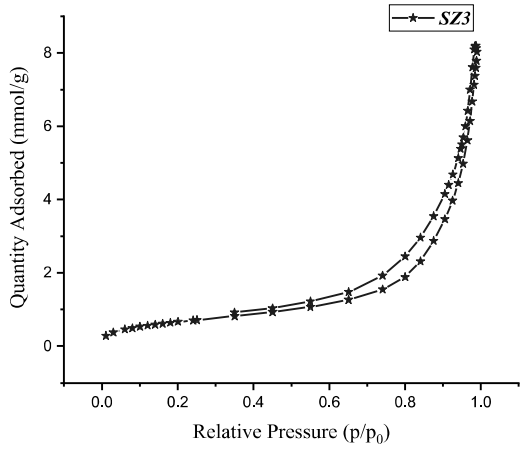
SZ3
Quantity Adsorbed (mmol/g)
Relative Pressure (p/p0)

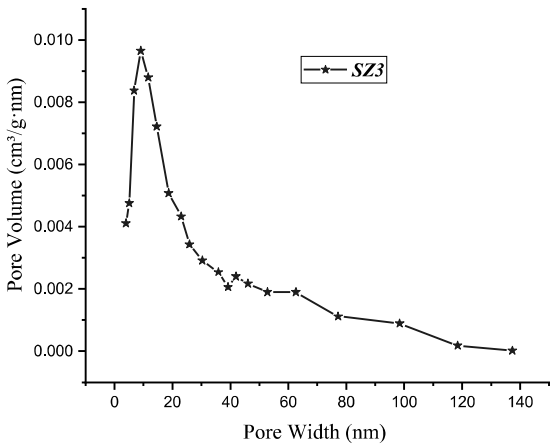
SZ3
Pore Volume (cm3/g·nm)
Pore Width (nm)

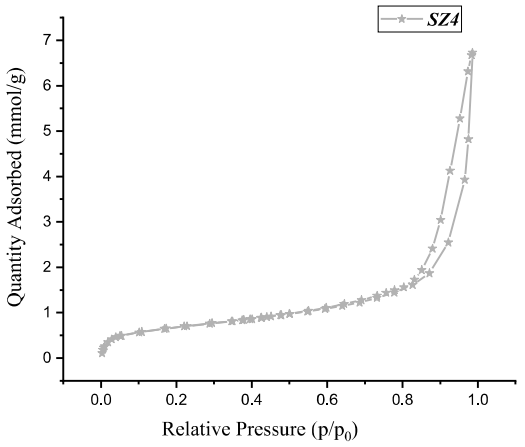
SZ4
Quantity Adsorbed (mmol/g)
Relative Pressure (p/p0)

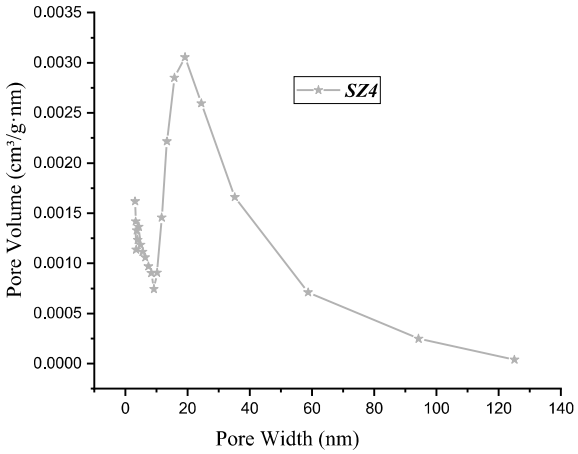
SZ4
Pore Volume (cm3/g·nm)
Pore Width (nm)

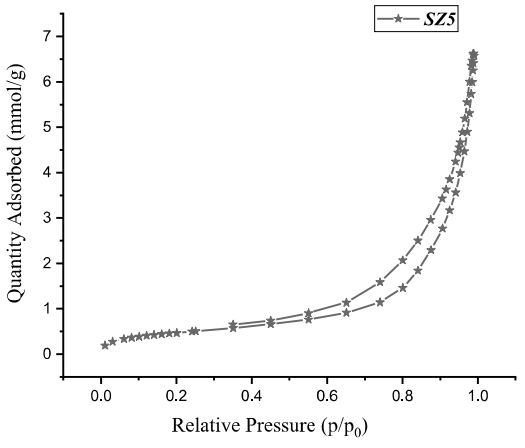
SZ5
Quantity Adsorbed (mmol/g)
Relative Pressure (p/p0)

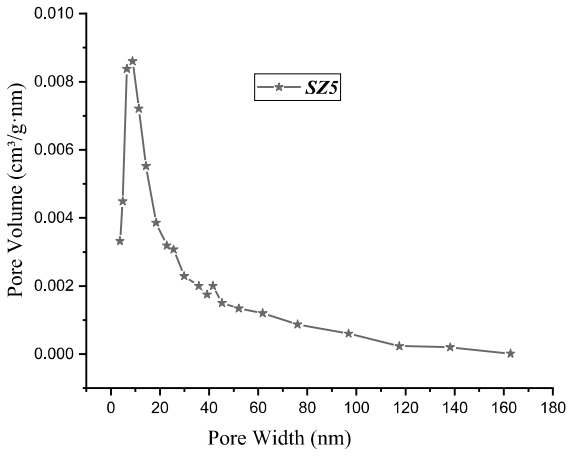
SZ5
Pore Volume (cm3/g·nm)
Pore Width (nm)

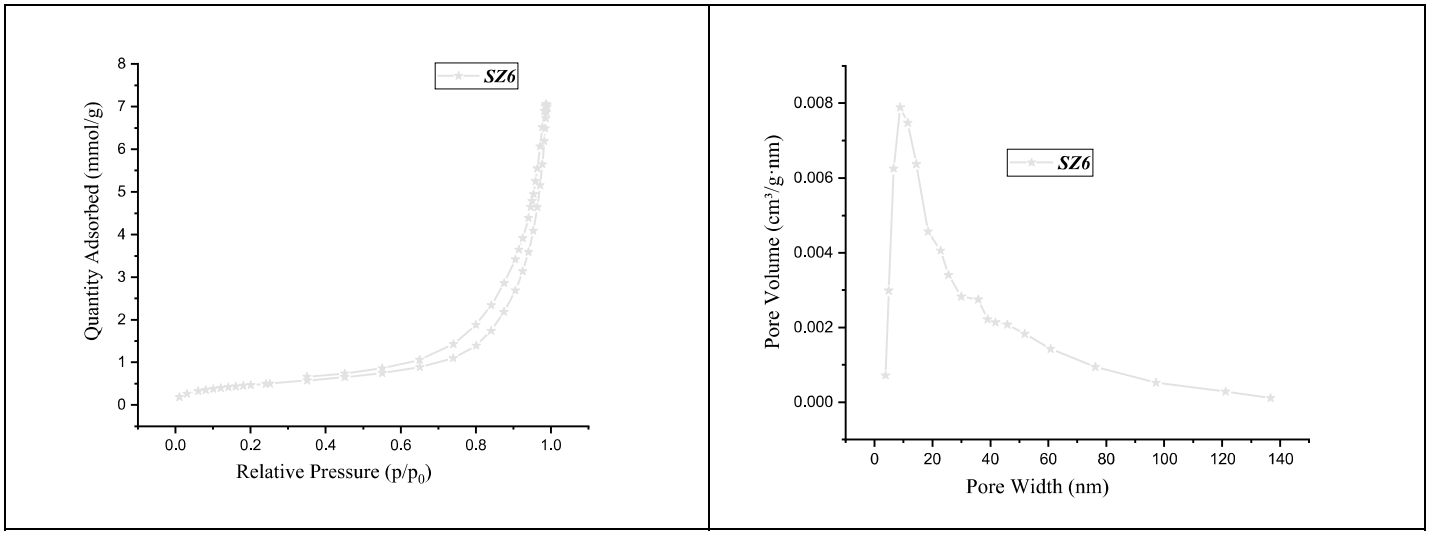

Fig. 8. Nitrogen adsorption/desorption models (a) and pore size distribution (b) of the Pristine HNC and the grafted HNC samples in several dispersing media.

Table 3. Brunauer–Emmett–Teller (BET) surface area, Barrett-Joyner-Halenda (BJH) pore volume and the average pore diameter for pristine HNC and the samples which were performed in the presence of several types of solvent.

Samples	**BET surface area (m^2/g)**	**BJH pore volume (cm^3/g)**	**Average pore diameter (nm)**
Pristine Halloysite	65.3	0.266	10
SZ1	8.6	0.07	18.9
SZ2	17.9	0.123	12.2
SZ3	55.7	0.256	9.1
SZ4	23.6	0.144	17.6
SZ5	39	0.207	6.5
SZ6	38.8	0.224	8.9

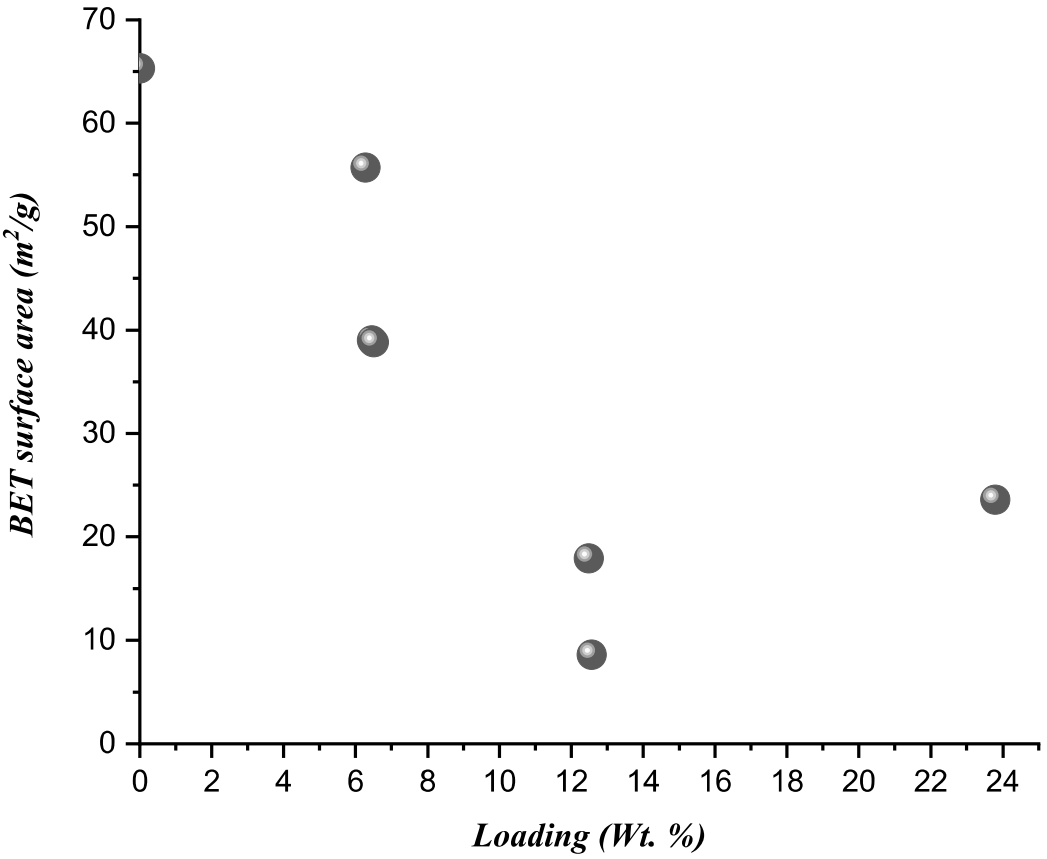

Fig. 9. Correlation between BET surface area and loading wt.%.

4. Conclusions

HNC has been chemically grafted by the use of GOPTMS in the presence of polar protic solvents (Ethanol), polar aprotic solvents (Tetrahydrofuran (THF) and Acetonitrile) and non-polar solvents (Hexane, 1,4-Dioxane and Toluene) as dispersing solvent. The greatest grade of grafting was obtained using Hexane as a solvent for the functionalization process. This highlights that the solvent properties (polarity and dielectric constant) are crucial in the silanization process. Non-polar solvents and the solvents with low values of dielectric constant are more appropriate for the silanization process because of their ability to facilitate interaction and condensation of silane molecules with the hydroxyl groups on HNC surfaces. As concerns polar protic solvents with large dielectric constant (such as Ethanol), the silane molecules resort to form hydrogen bond with the solvent rather than to condensate with the hydroxyl groups on HNC surfaces. On the other hand, Non-

polar solvents with low values of dielectric constant such as n- Hexane, the silane molecules tend to condensate with the hydroxyl groups on HNC surface and don't form H-bonding with the solvent. This study provides a guide on the impact of the solvent on the proceeding of the silanization process.

Conflicts of interest

The authors declare that they have no known competing financial interests to influence the work reported in this paper.

Acknowledgements

This work was supported by the Program 211 of the Government of the Russian Federation, RFBR grants 17-03-00641 and 18-29- 12129mk, the State Task from the Ministry of the Education and Science of the Russian Federation.

Reference

1. B. Sarkar, R. Rusmin, U. C. Ugochukwu, R. Mukhopadhyay, and K. M. Manjaiah, *Modified Clay Minerals for Environmental Applications* (Elsevier Inc., 2018).
2. Y. Lvov, A. Aerov, and R. Fakhrullin, Advances in Colloid and Interface Science **207**, 189 (2014).
3. Y. M. Lvov, M. M. DeVilliers, and R. F. Fakhrullin, Expert Opinion on Drug Delivery **13**, 977 (2016).
4. M. Fizir, P. Dramou, N. S. Dahiru, W. Ruya, T. Huang, and H. He, Microchim Acta **185**, 389 (2018).
5. L. Lisuzzo, G. Cavallaro, F. Parisi, S. Milioto, and G. Lazzara, Ceramics International **45**, 2858 (2019).
6. A. M. Abu El-Soad, M. I. Sayyed, K. A. Mahmoud, E. Şakar, and E. G. Kovaleva, Journal of Radiation Research and Applied Sciences, **13**, 94 (n.d.).
7. H. He, Q. Tao, J. Zhu, P. Yuan, W. Shen, and S. Yang, Applied Clay Science **71**, 15 (2013).
8. M. Massaro, G. Lazzara, S. Milioto, R. Noto, and S. Riela, J. Mater. Chem. B **5**, 2867 (2017).
9. M. Connolly, Y. Zhang, S. Mahri, D. M. Brown, N. Ortuño, M. Jordá-Beneyto, K. Maciaszek, V. Stone, T. F. Fernandes, and H. J. Johnston, Food and Chemical Toxicology **126**, 178 (2019).
10. J. Kalaiyarasi, S. Meenakshi, S. C. B. Gopinath, and K. Pandian, Microchim Acta **184**, 4485 (2017).
11. D. Tan, P. Yuan, F. Annabi-Bergaya, H. Yu, D. Liu, H. Liu, and H. He, Microporous and Mesoporous Materials **179**, 89 (2013).
12. G. Cavallaro, L. Chiappisi, P. Pasbakhsh, M. Gradzielski, and G. Lazzara, Applied Clay Science **160**, 71 (2018).
13. A. M. Abu El-Soad, M. I. Sayyed, K. A. Mahmoud, E. Şakar, and E. G. Kovaleva, Applied Radiation and Isotopes **154**, 108882 (2019).
14. A. Maleki, Z. Hajizadeh, and R. Firouzi-Haji, Microporous and Mesoporous Materials **259**, 46 (2018).
15. G. I. Fakhrullina, F. S. Akhatova, Y. M. Lvov, and R. F. Fakhrullin, Environ. Sci.: Nano **2**, 54 (2015).
16. M. Kryuchkova, A. Danilushkina, Y. Lvov, and R. Fakhrullin, Environ. Sci.: Nano **3**, 442 (2016).
17. C. R. Kaze, H. K. Tchakoute, T. T. Mbakop, J. R. Mache, E. Kamseu, U. C. Melo, C. Leonelli, and H. Rahier, Ceramics International **44**, 18499 (2018).
18. G. Tian, W. Wang, B. Mu, Q. Wang, and A. Wang, Ceramics International **43**, 1862 (2017).
19. L. Lisuzzo, G. Cavallaro, P. Pasbakhsh, S. Milioto, and G. Lazzara, Journal of Colloid and Interface Science **547**, 361 (2019).

20. Z. Qin, Y. Jiang, H. Piao, S. Tao, Y. Sun, X. Wang, P. Ma, and D. Song, Microchimica Acta **186**, 489 (2019).
21. D. Tan, P. Yuan, D. Liu, and P. Du, *Surface Modifications of Halloysite* (2016).
22. D. Tan, H. Zhang, S. Sun, F. Dong, H. Sun, and B. Li, Applied Clay Science **177**, 37 (2019).
23. M. Alkan, G. Tekin, and H. Namli, Microporous and Mesoporous Materials **84**, 75 (2005).
24. P. Pasbakhsh, G. J. Churchman, and J. L. Keeling, Appl. Clay Sci. **74**, 47 (2013).
25. E. Bischoff, T. Daitx, D. A. Simon, H. S. Schrekker, S. A. Liberman, and R. S. Mauler, Applied Clay Science **112–113**, 68 (2015).
26. Q. Zhang, Q. Liu, Y. Zhang, H. Cheng, and Y. Lu, Applied Clay Science **65–66**, 134 (2012).
27. A. M. Abu El-Soad, A. V. Pestov, D. P. Tambasova, V. A. Osipova, N. A. Martemyanov, G. Cavallaro, E. G. Kovaleva, and G. Lazzara, Journal of Organometallic Chemistry **915**, (2020).
28. I. Blanco, G. Cicala, A. Latteri, G. Saccullo, A. M. M. El-Sabbagh, and G. Ziegmann, Journal of Thermal Analysis and Calorimetry **127**, 147 (2017).
29. I. Blanco, L. Abate, F. A. Bottino, and P. Bottino, Polymer Degradation and Stability **102**, 132 (2014).
30. S. Cataldo, G. Lazzara, M. Massaro, N. Muratore, A. Pettignano, and S. Riela, Applied Clay Science **156**, 87 (2018).
31. S. Rooj, A. Das, V. Thakur, R. N. Mahaling, A. K. Bhowmick, and G. Heinrich, Materials and Design **31**, 2151 (2010).
32. Z. Wang, H. Wang, J. Liu, and Y. Zhang, Desalination **344**, 313 (2014).
33. H. Fu, Y. Wang, X. Li, and W. Chen, Composites Science and Technology **126**, 86 (2016).
34. George Socrates, *Infrared and Raman Characteristic Group Frequencies Contents* (2001).
35. L. Andrini, R. M. Toja, M. S. Conconi, F. G. Requejo, and N. M. Rendtorff, Journal of Electron Spectroscopy and Related Phenomena **234**, 19 (2019).
36. M. Liu, Z. Jia, D. Jia, and C. Zhou, Progress in Polymer Science **39**, 1498 (2014).
37. M. J. Saif, M. Naveed, K. M. Zia, and M. Asif, Radiation Physics and Chemistry **127**, 115 (2016).
38. V. Akbari, F. Najafi, H. Vahabi, M. Jouyandeh, M. Badawi, S. Morisset, M. R. Ganjali, and M. R. Saeb, Progress in Organic Coatings **135**, 555 (2019).
39. K. K. Sharma, A. Anan, R. P. Buckley, W. Ouellette, and T. Asefa, Journal of the American Chemical Society **130**, 218 (2008).
40. T. W. Bentley, D. N. Ebdon, E. J. Kim, and S. K. In, Journal of Organic Chemistry. **70**, 1647 (2005).
41. J. Y. Kim, D. O. Shin, T. Chang, K. M. Kim, J. Jeong, J. Park, Y. M. Lee, K. Y. Cho, C. Phatak, S. Hong, and Y. G. Lee, Electrochimica Acta **300**, 299 (2019).
42. M. Belmares, M. Blanco, W. A. Goddard, R. B. Ross, G. Caldwell, S. H. Chou, J. Pham, P. M. Olofson, and C. Thomas, Journal of Computational Chemistry **25**, 1814 (2004).
43. A. K. Panda, B. G. Mishra, D. K. Mishra, and R. K. Singh, Colloids and Surfaces A : Physicochemical and Engineering Aspects **363**, 98 (2010).
44. C. Sangwichien, G. L. Aranovich, and M. D. Donohue, Colloids and Surfaces A: Physicochemical and Engineering Aspects **206**, 313 (2002).

Figure captions

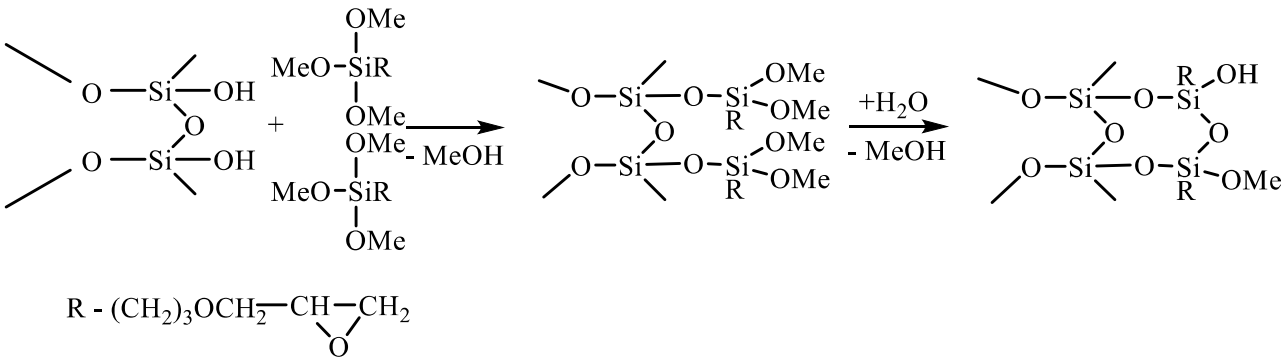

Fig. 1. The sketch for chemical grafting of GOPTMS on HNC surface.

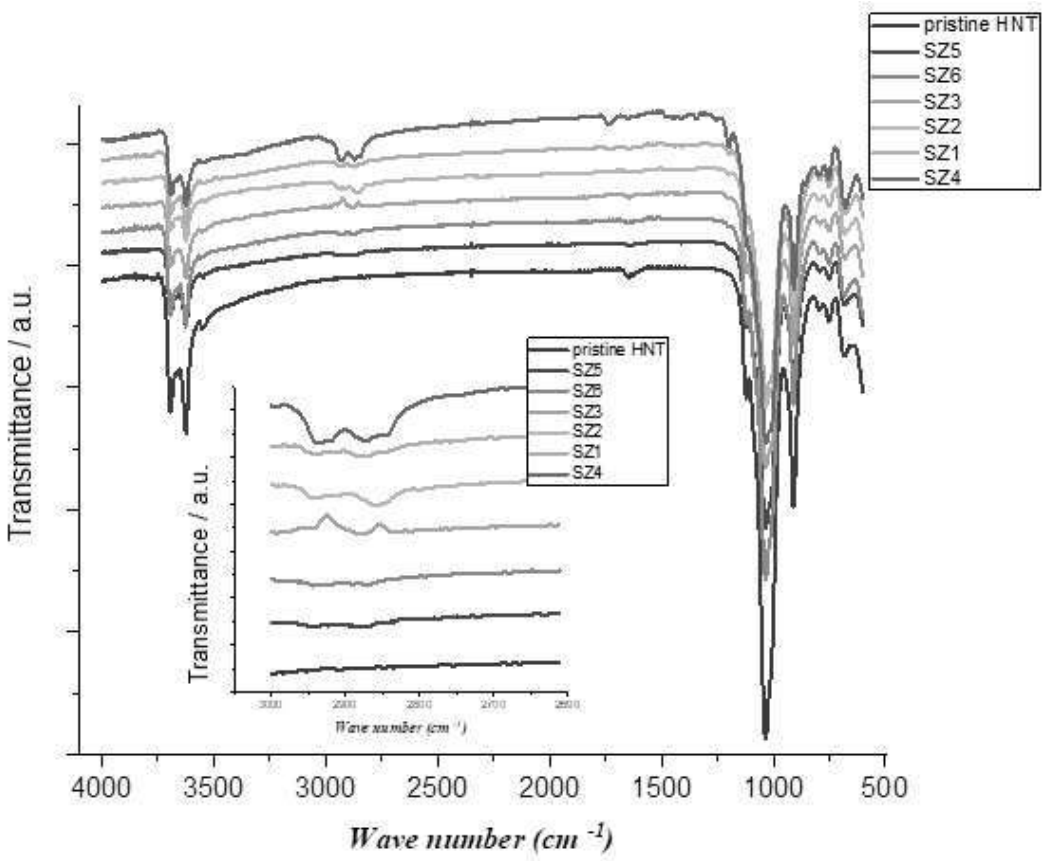

Fig. 2. FT-IR spectra for pristine HNC and HNC samples which are grafted by GOPTMS in the presence of several types of solvents.

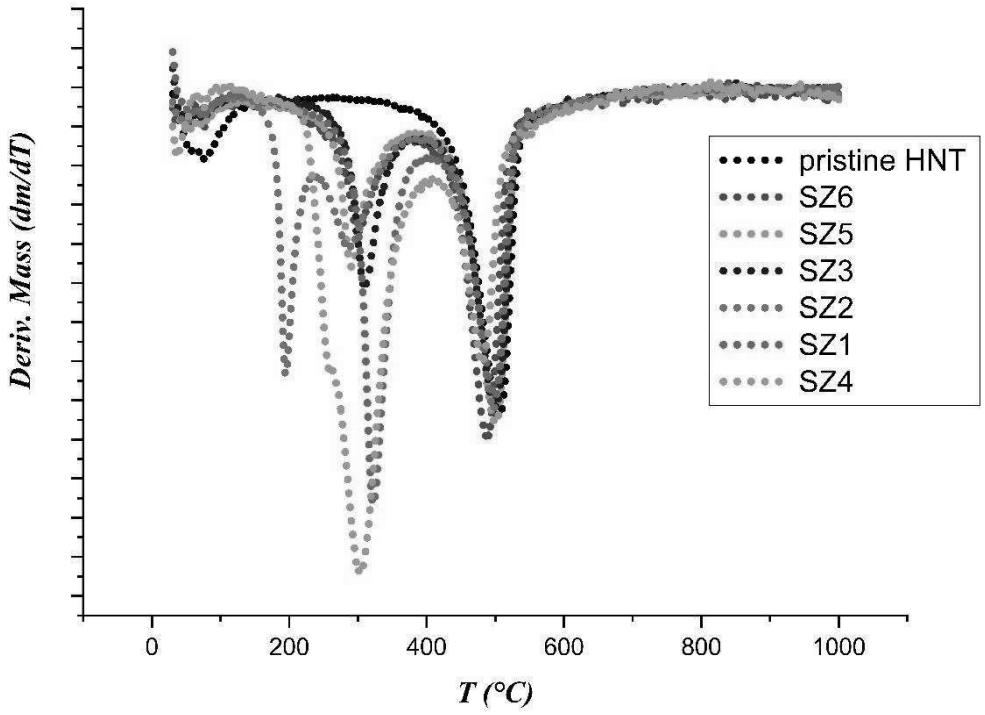

Fig. 3. DTG curves of pristine HNC and grafted HNC samples in the presence of several dispersing media.

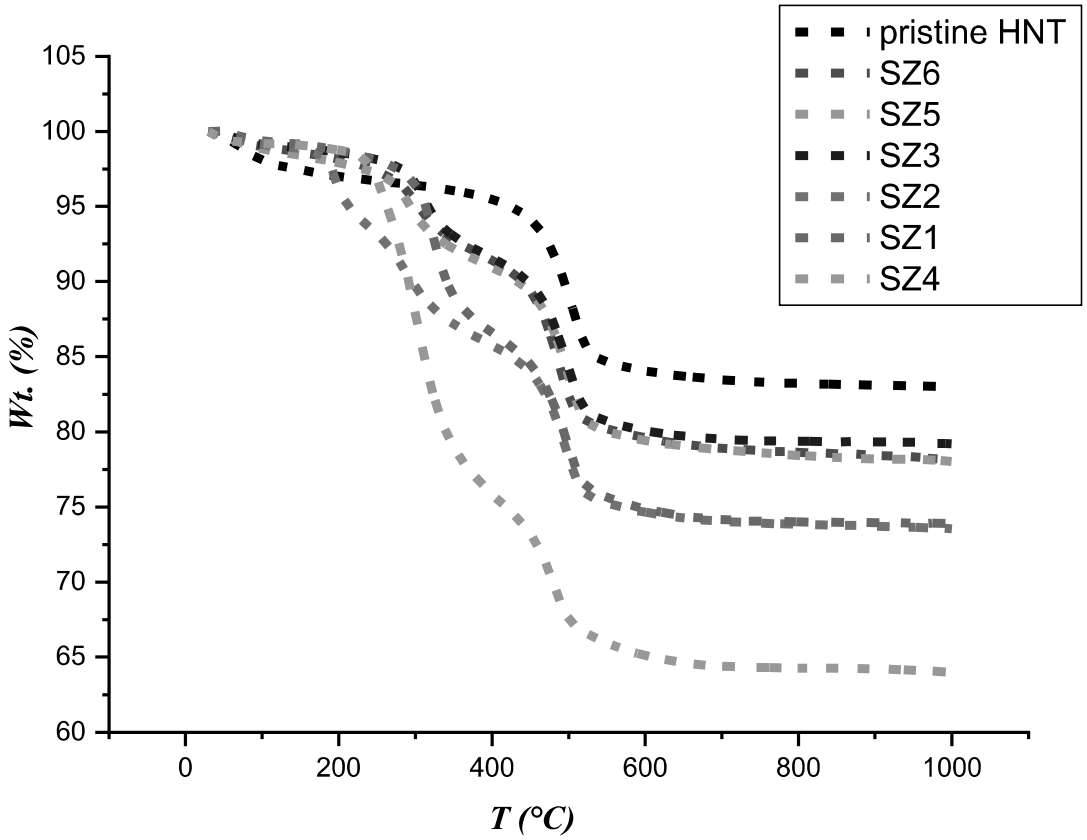

Fig. 4. Thermogravimetric analysis of pristine HNC and grafted HNC samples in the presence of several dispersing media.

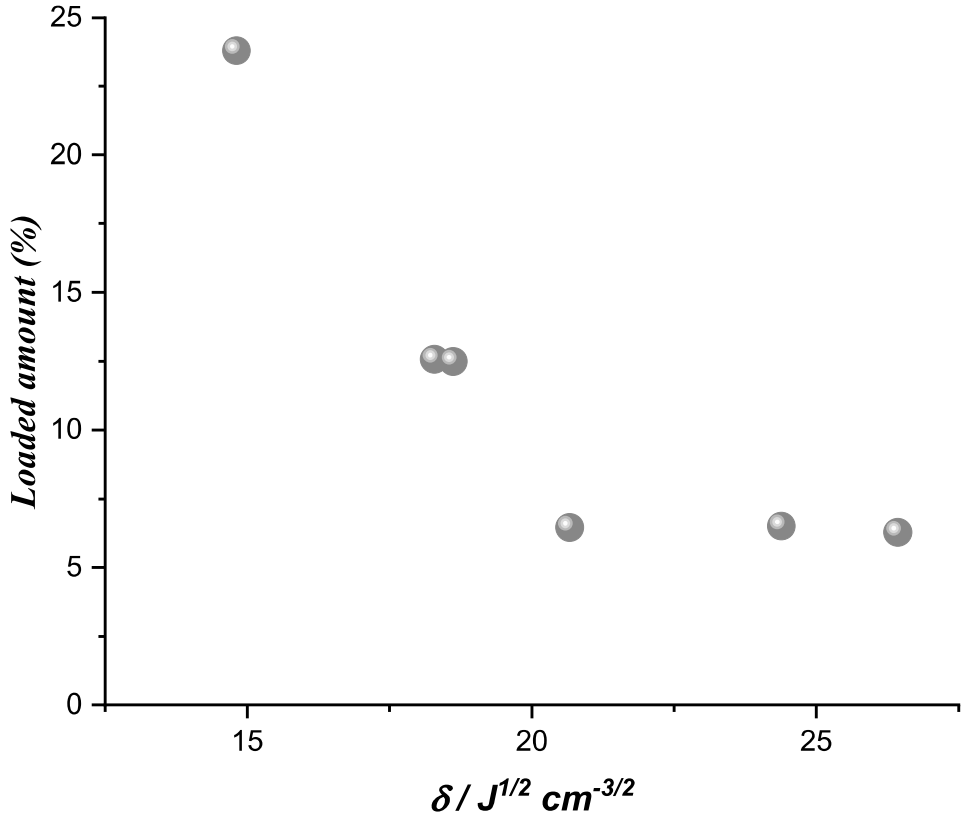

Fig. 5. The relation between Wt. (%) of silane loaded and the solubility parameters.

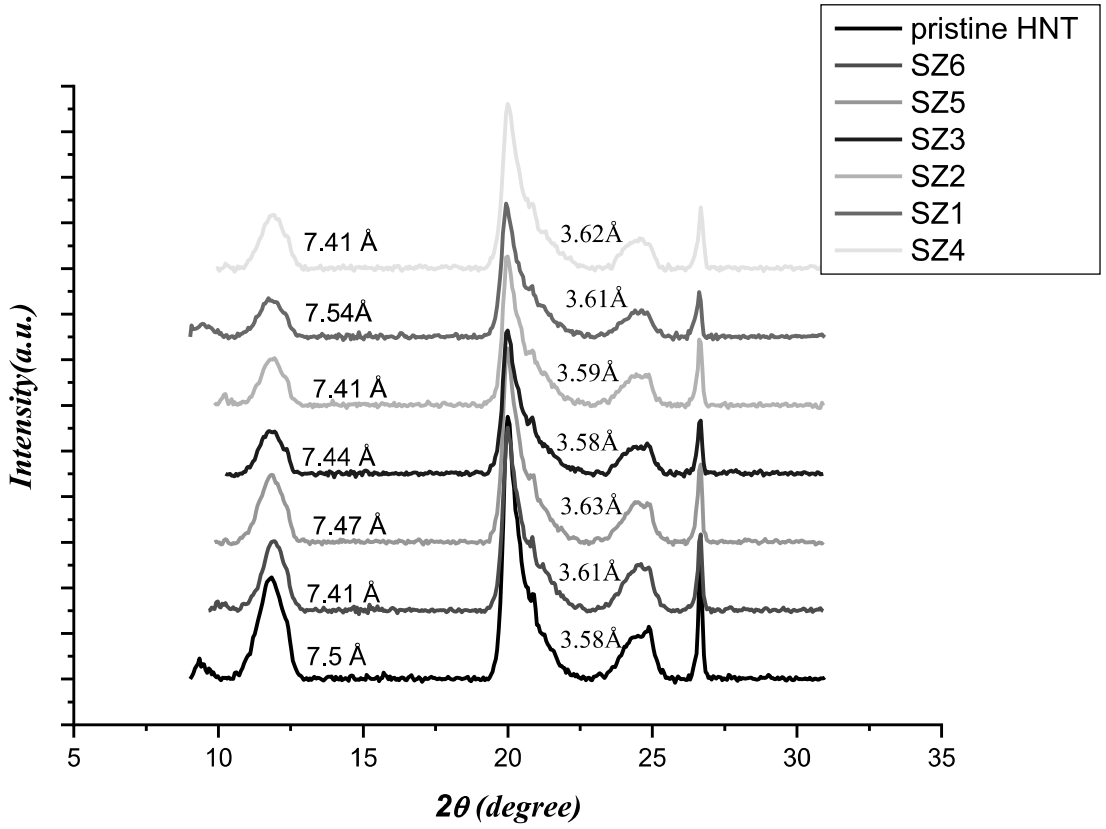

Fig. 6. XRD patterns of pristine HNC and grafted HNC samples in the presence of several dispersing media.

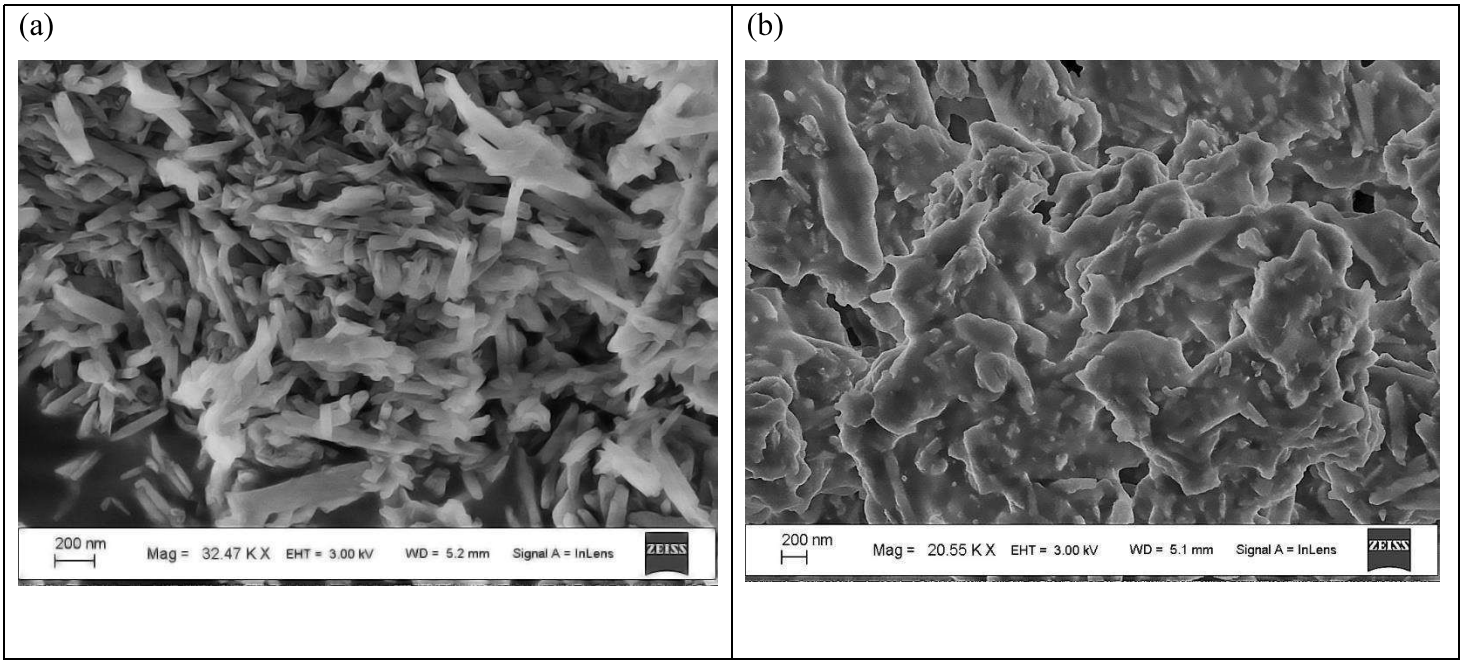

Fig. 7. SEM images for pristine HNC (a) and SZ4 sample (b).

(a)

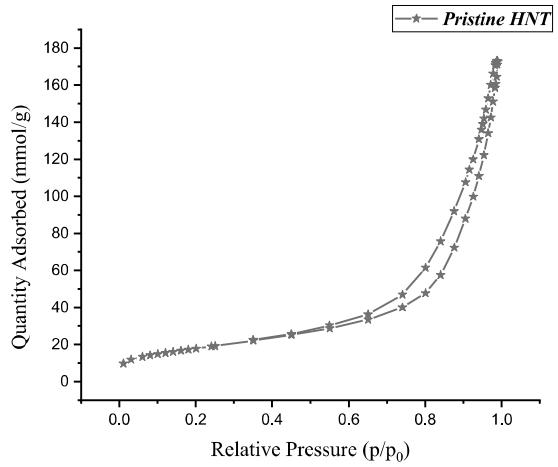
Pristine HNT
Quantity Adsorbed (mmol/g)
Relative Pressure (p/p0)

(b)

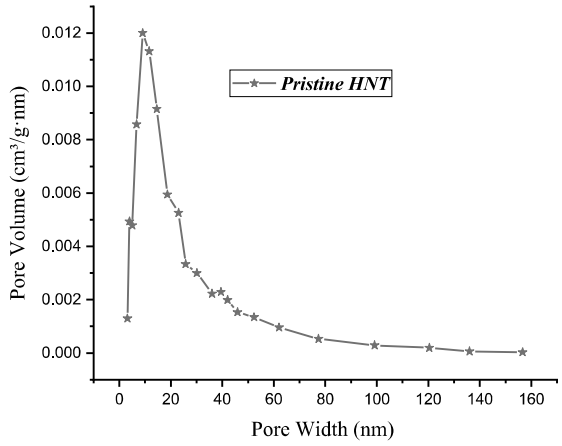
Pristine HNT
Pore Volume (cm3/g·nm)
Pore Width (nm)

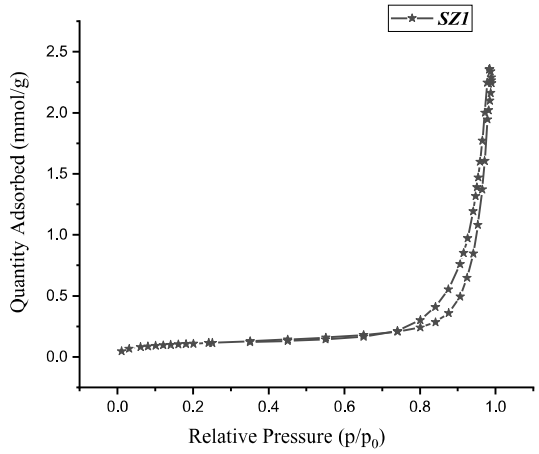
SZ1
Quantity Adsorbed (mmol/g)
Relative Pressure (p/p0)

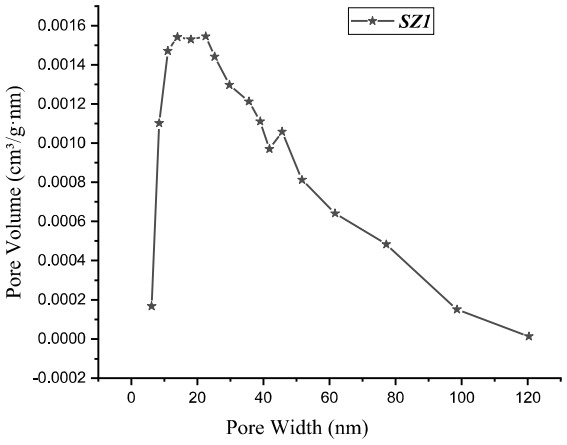
SZ1
Pore Volume (cm3/g·nm)
Pore Width (nm)

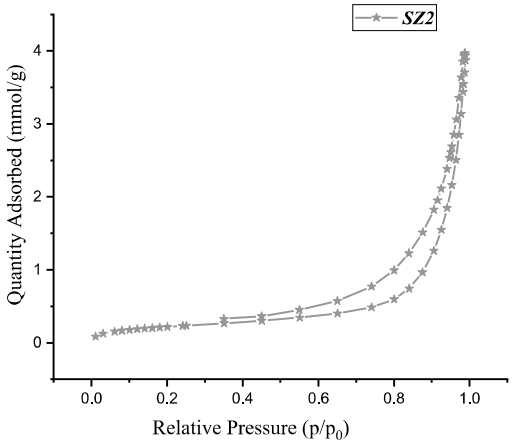
SZ2
Quantity Adsorbed (mmol/g)
Relative Pressure (p/p0)

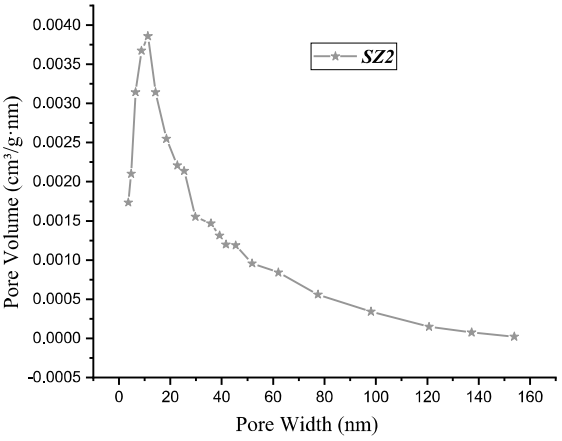
SZ2
Pore Volume (cm3/g·nm)
Pore Width (nm)

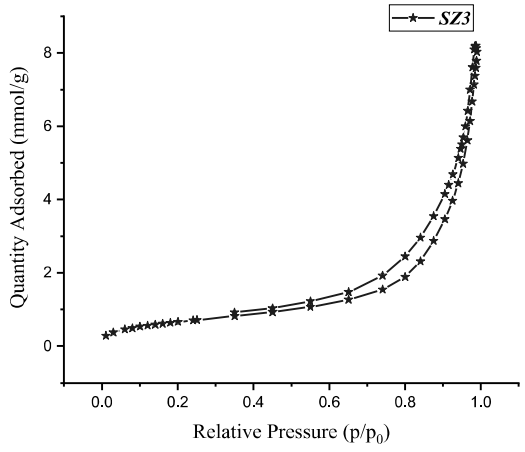
SZ3
Quantity Adsorbed (mmol/g)
Relative Pressure (p/p0)

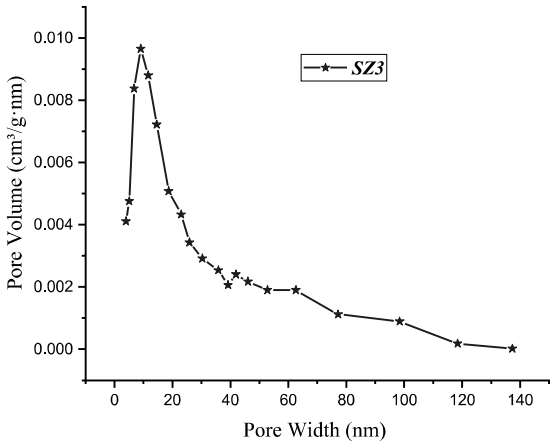
SZ3
Pore Volume (cm3/g·nm)
Pore Width (nm)

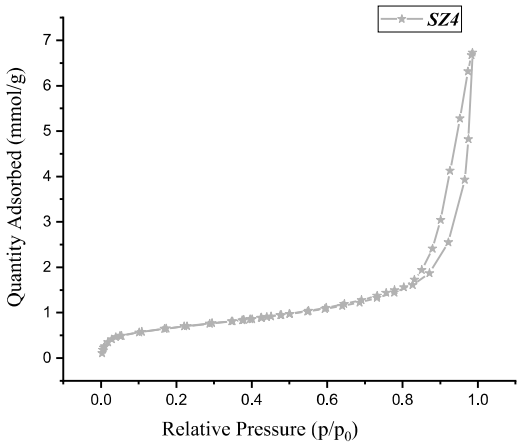
SZ4
Quantity Adsorbed (mmol/g)
Relative Pressure (p/p0)

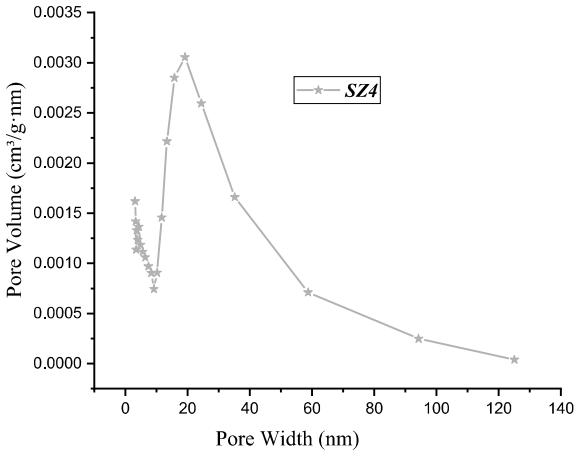
SZ4
Pore Volume (cm3/g·nm)
Pore Width (nm)

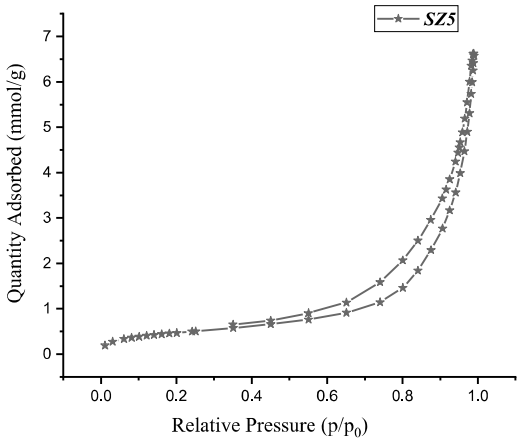
SZ5
Quantity Adsorbed (mmol/g)
Relative Pressure (p/p0)

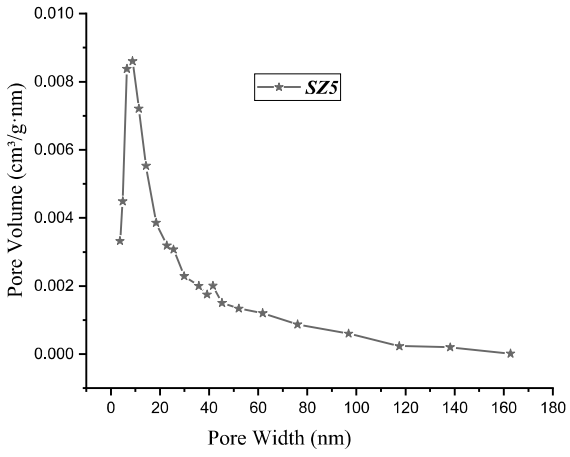
SZ5
Pore Volume (cm3/g·nm)
Pore Width (nm)

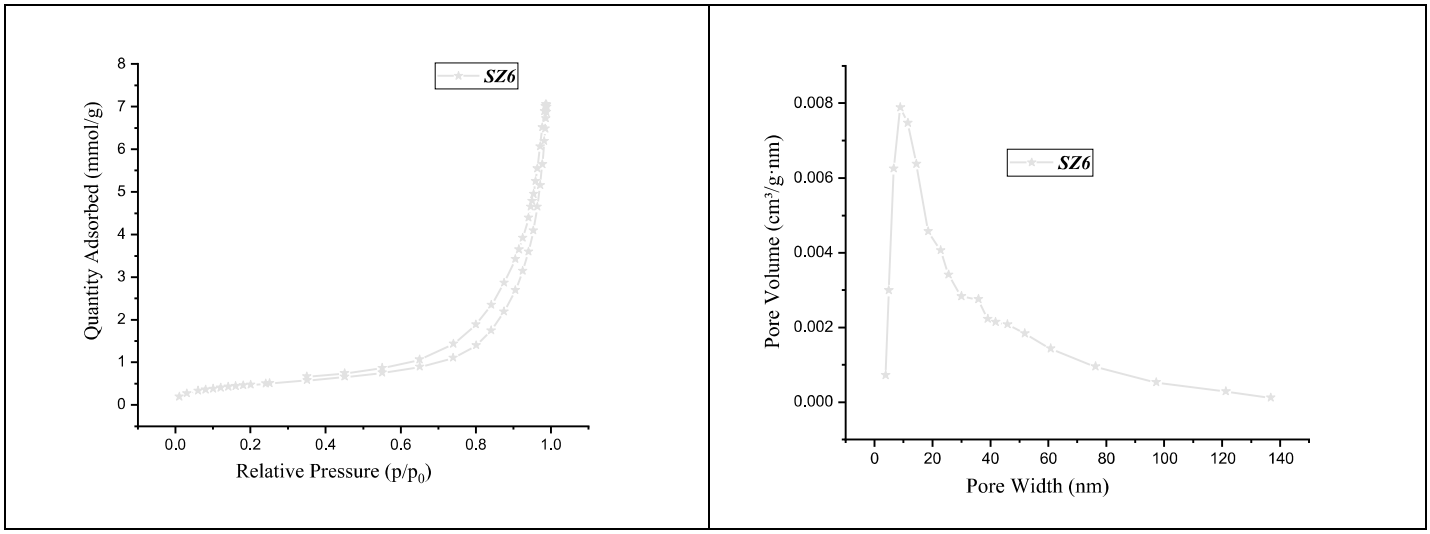

Fig. 8. Nitrogen adsorption/desorption models (a) and pore size distribution (b) of the Pristine HNC and the grafted HNC samples in several dispersing media.

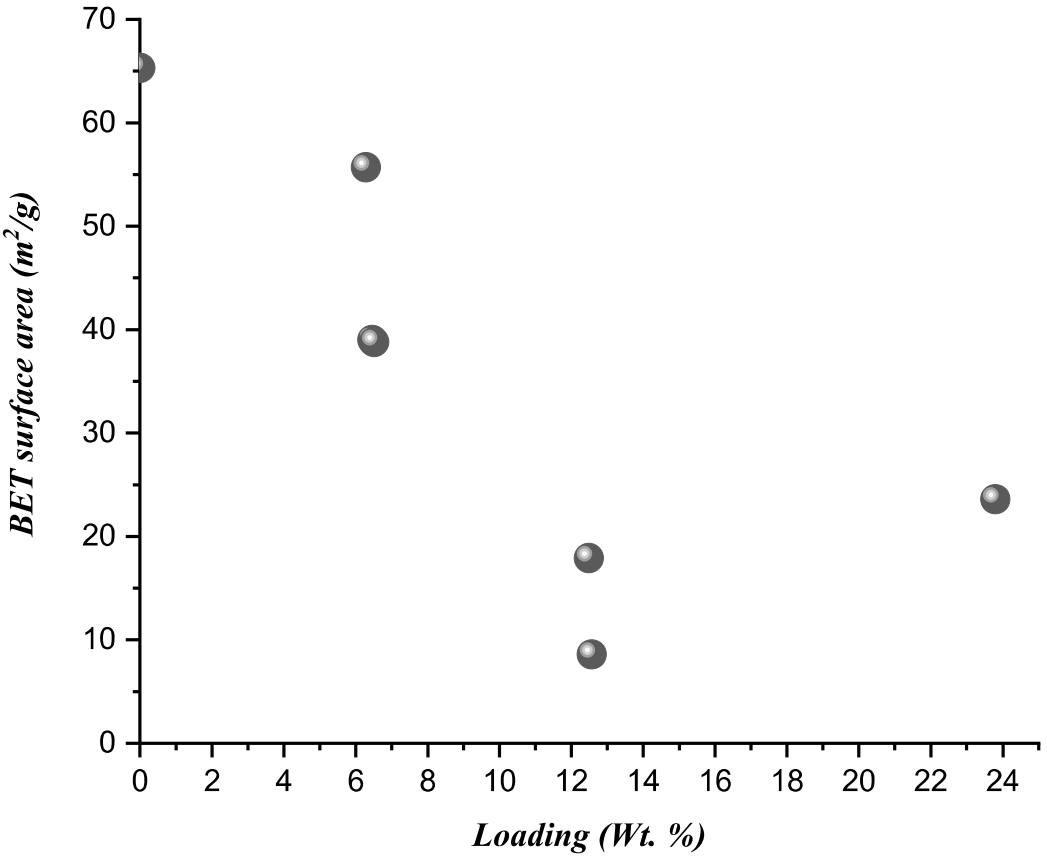

Fig. 9. Correlation between BET surface area and loading wt.%.

List of tables

Table 1. Elemental analysis of HNC samples which have been chemically grafted in various types of solvent using the trifunctional organosilane agent [GOPTMS].

Sample	Content, %			Solvent	Degree of functionalization %
	C	H	N		
SZ1	8.98	2.73	0.00	Toluene	45.6
SZ2	8.56	2.66	0.00	THF	43.5
SZ3	4.56	2.19	0.00	Ethanol	23.2
SZ4	18.31	3.9	0.00	n-Hexane	93.3
SZ5	4.12	2.15	0.00	1, 4 dioxane	21.0
SZ6	4.12	2.12	0.00	Acetonitrile	21.0

Table 2. Thermogravimetric analysis of HNC samples which have been grafted in several types of solvent using (3-glycidyloxypropyl) trimethoxy silane.

Sample	Solvent	Dielectric constant	δ / $J^{1/2}$ $cm^{-3/2}$	Loaded amount (%) [a]
SZ1	Toluene	2.4	18.29	12.57
SZ2	THF	7.5	18.62	12.49
SZ3	Ethanol	24.5	26.43	6.28
SZ4	n-Hexane	2.0	14.81	23.80
SZ5	1, 4 dioxane	2.3	20.66	6.46
SZ6	Acetonitrile	37.5	24.39	6.51

[a] Determined by using Eq. (2)

Table 3. Brunauer–Emmett–Teller (BET) surface area, Barrett-Joyner-Halenda (BJH) pore volume and the average pore diameter for pristine HNC and the samples which were performed in the presence of several types of solvent.

Samples	BET surface area (m^2/g)	BJH pore volume (cm^3/g)	Average pore diameter (nm)
Pristine Halloysite	65.3	0.266	10
SZ1	8.6	0.07	18.9
SZ2	17.9	0.123	12.2
SZ3	55.7	0.256	9.1
SZ4	23.6	0.144	17.6
SZ5	39	0.207	6.5
SZ6	38.8	0.224	8.9

Abstract

The grafting of silane groups on clay surfaces has been recently investigated in order to fabricate versatile compounds with new potential applications in materials science and ecological engineering. This work inspected the influence of variety of solvents on the silanization of halloysite nanoclay (HNC) surface by (3-Glycidyloxy propyl) trimethoxy silane. Functionalization of halloysite nanoclay (HNC) by 3-Glycidyloxypropyltrimethoxysilane (GOPTMS) has been performed in polar protic solvents (Ethanol), polar aprotic solvents (Tetrahydrofuran (THF) and Acetonitrile) and non-polar solvents (Hexane, 1,4-Dioxane and Toluene) as dispersing media. The silane grafted materials were distinguished by using Fourier Transform Infrared Spectroscopy (FT-IR), elemental analysis, Scanning Electron Microscopy (SEM), Thermogravimetry (TGA), X-ray Diffraction Analysis (XRD) and Nitrogen adsorption/desorption isotherms. The greatest percent of the loaded silane was obtained by using Hexane as a solvent.

Keywords: Halloysite, solvent, solubility parameters, thermogravimetric analysis, FT-IR, XRD.

Cover letter

Dear Editor,

I am writing to express my interest in Journal of Inorganic and Organometallic Polymers and Materials.

It'll be a great pleasure to submit my article which entitled:

“Effect of polarity of solvent on silanization of halloysite nanoclay using (3-Glycidyloxy propyl) trimethoxy silane”

for peer review in your journal.

I will be very happy if you accept my paper.

With my best wishes

Asmaa

Figure captions

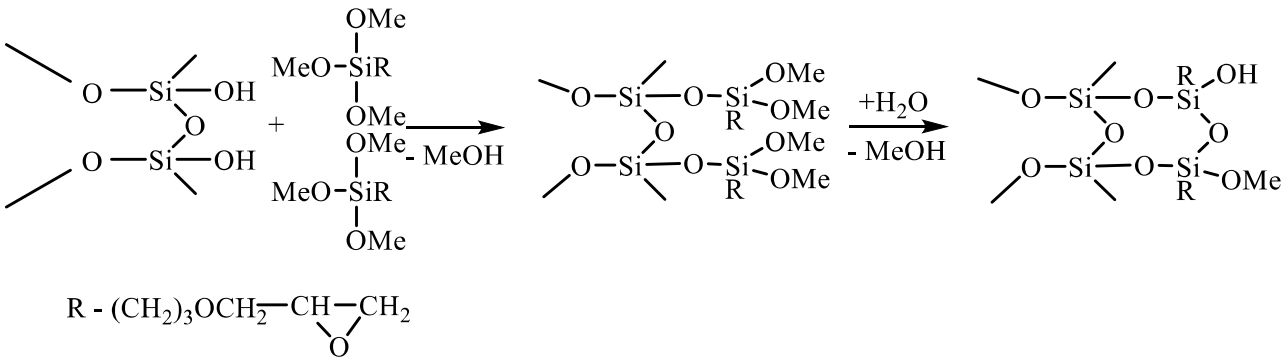

Fig. 1. The sketch for chemical grafting of GOPTMS on HNC surface.

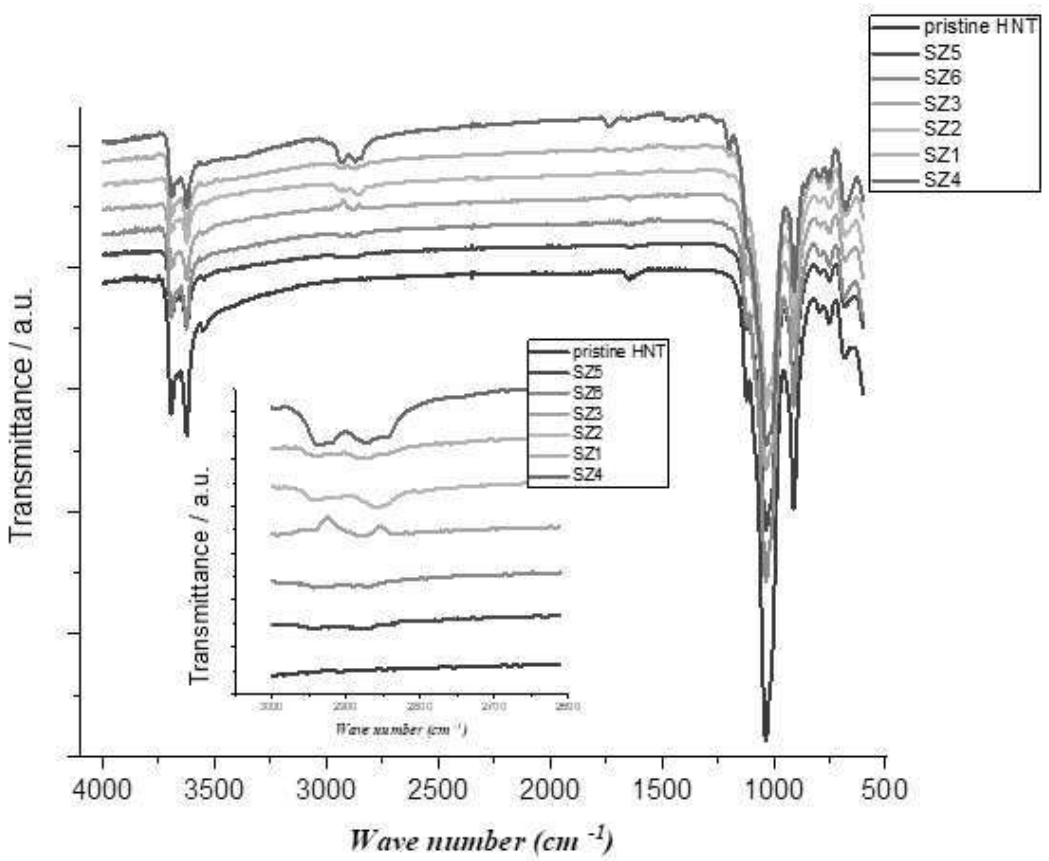

Fig. 2. FT-IR spectra for pristine HNC and HNC samples which are grafted by GOPTMS in the presence of several types of solvents.

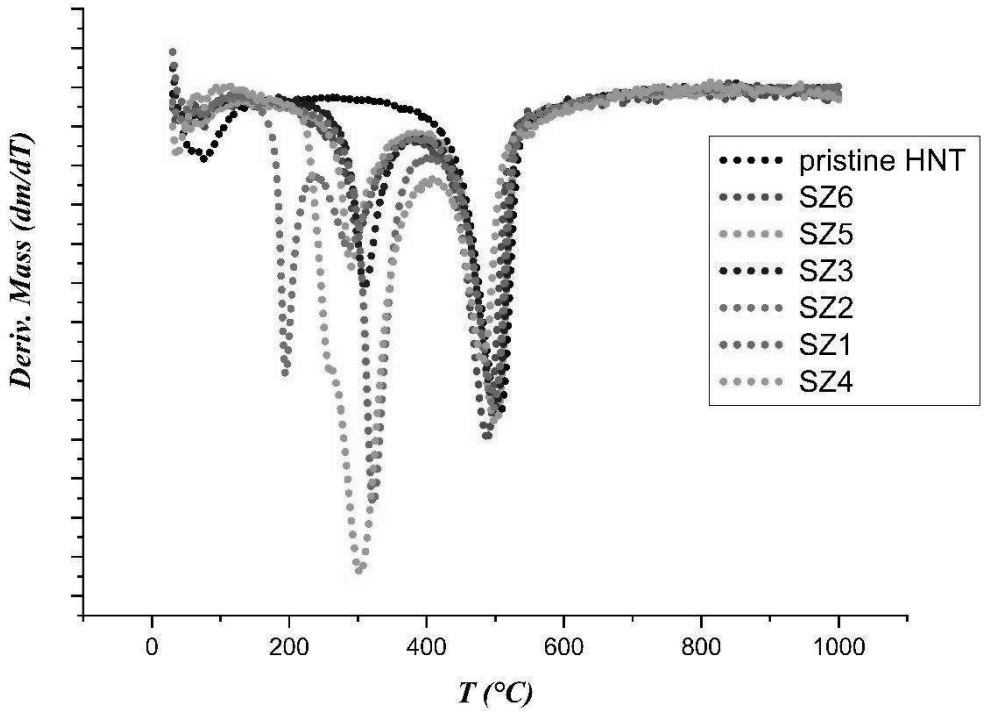

Fig. 3. DTG curves of pristine HNC and grafted HNC samples in the presence of several dispersing media.

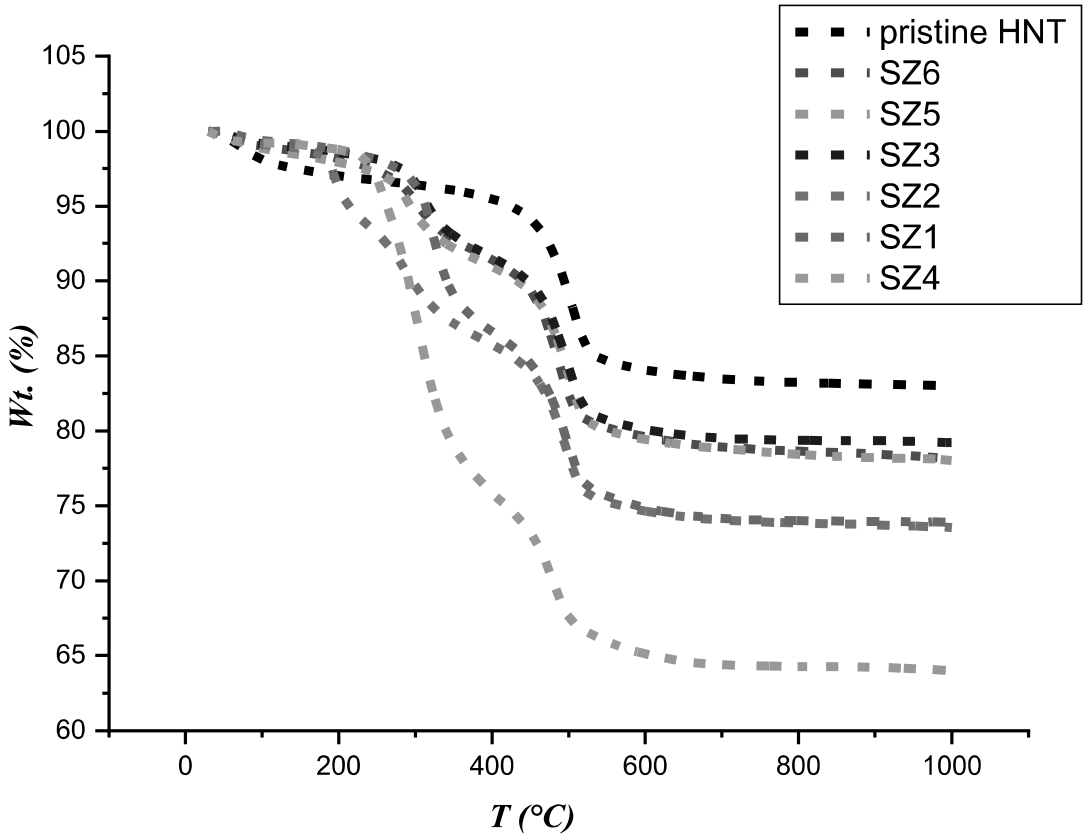

Fig. 4. Thermogravimetric analysis of pristine HNC and grafted HNC samples in the presence of several dispersing media.

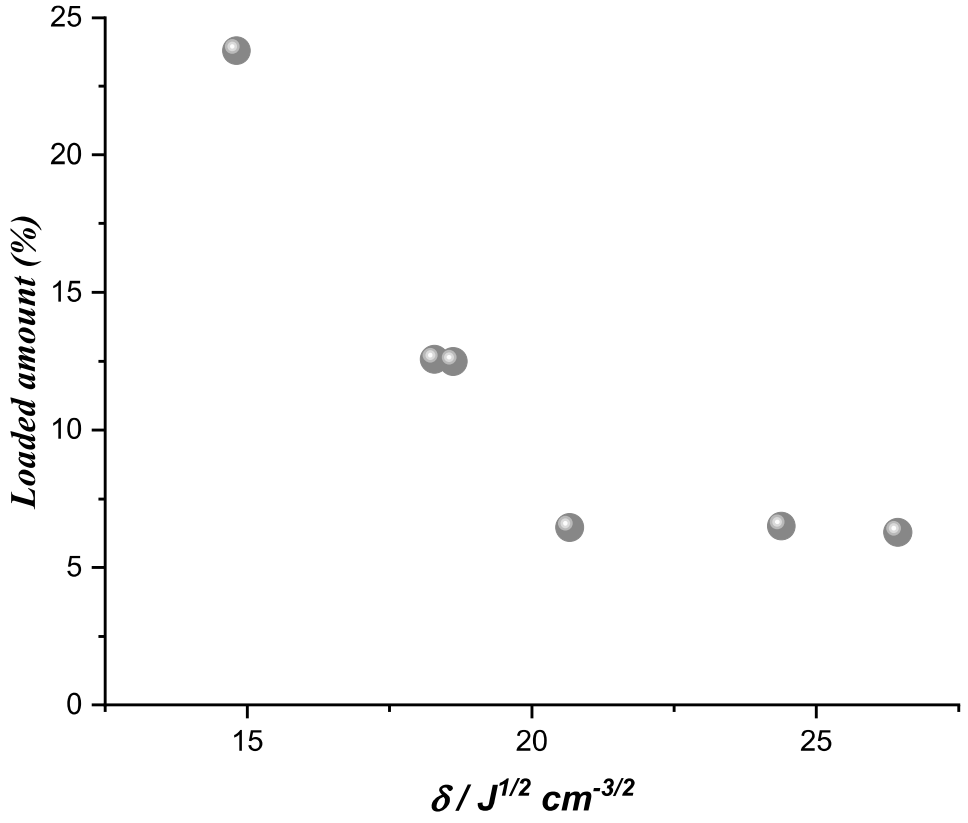

Fig. 5. The relation between Wt. (%) of silane loaded and the solubility parameters.

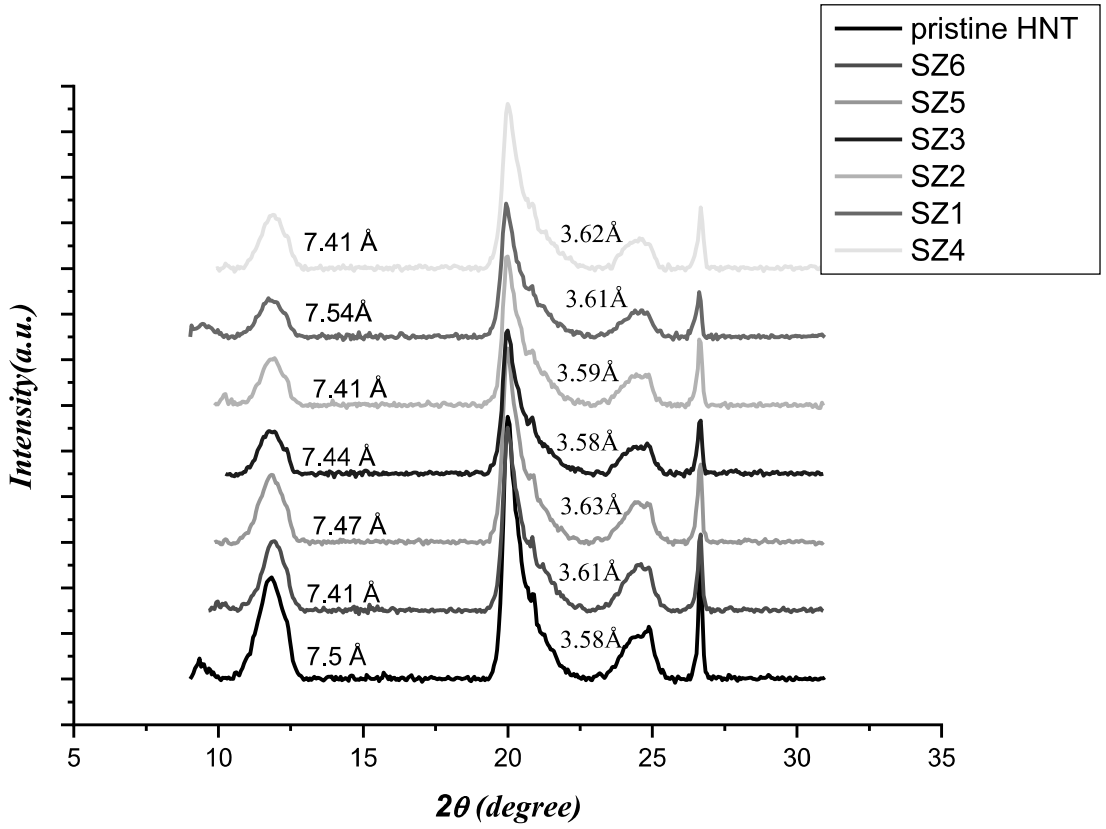

Fig. 6. XRD patterns of pristine HNC and grafted HNC samples in the presence of several dispersing media.

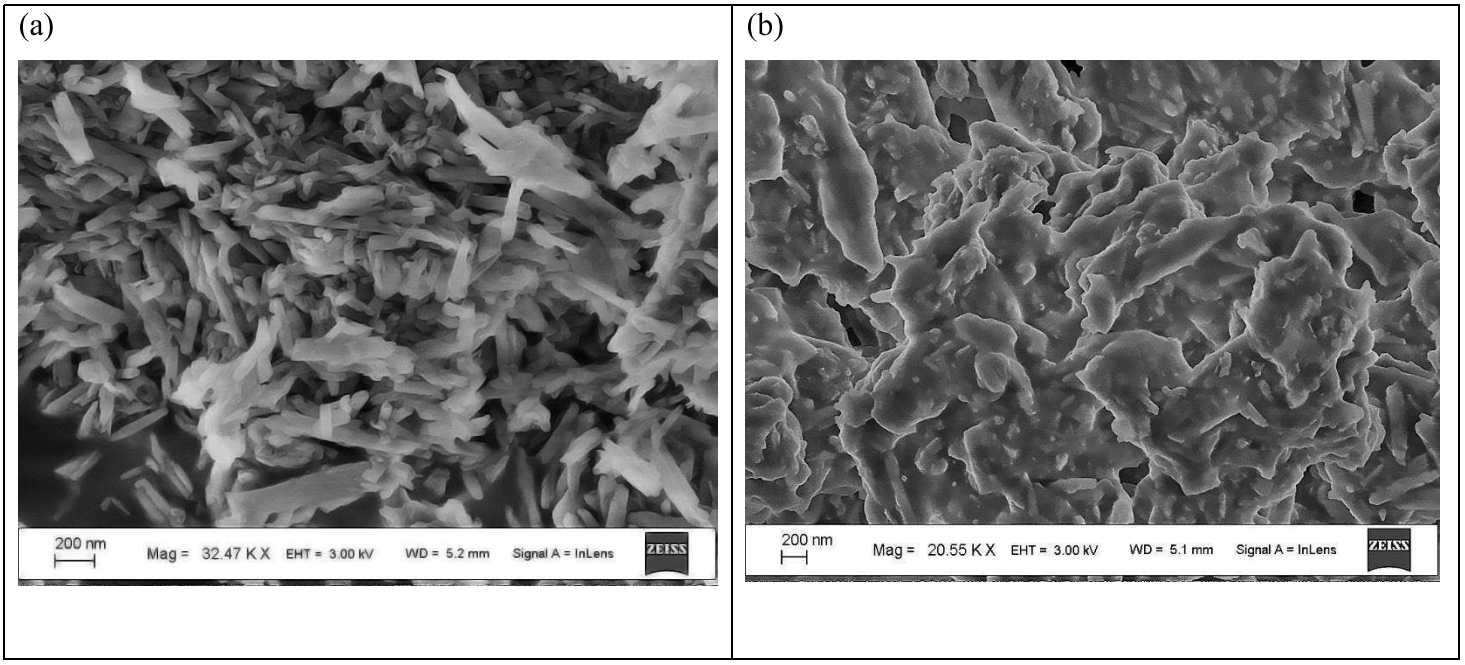

Fig. 7. SEM images for pristine HNC (a) and SZ4 sample (b).

(a)

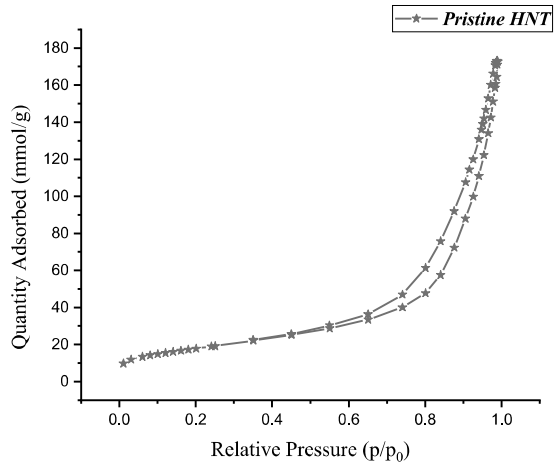
Pristine HNT
Quantity Adsorbed (mmol/g)
Relative Pressure (p/p0)

(b)

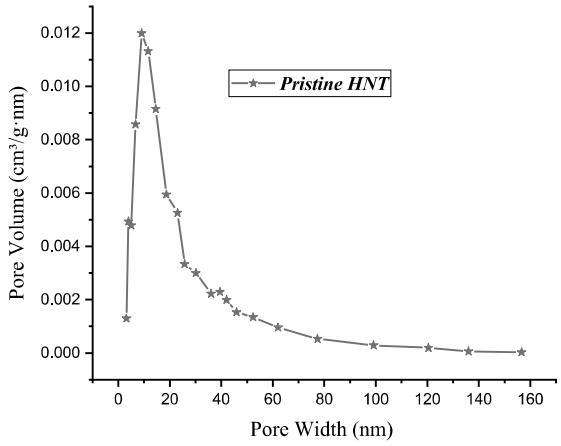
Pristine HNT
Pore Volume (cm3/g·nm)
Pore Width (nm)

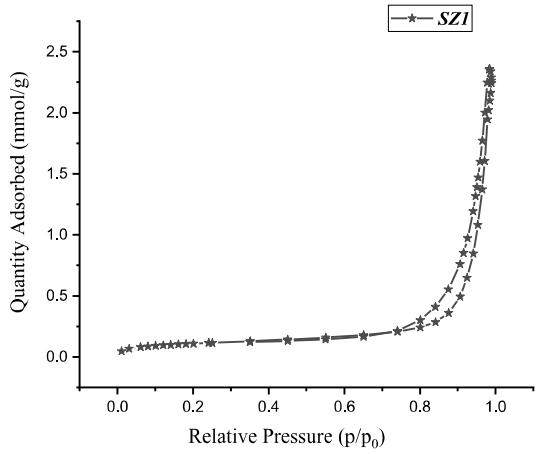
SZ1
Quantity Adsorbed (mmol/g)
Relative Pressure (p/p0)

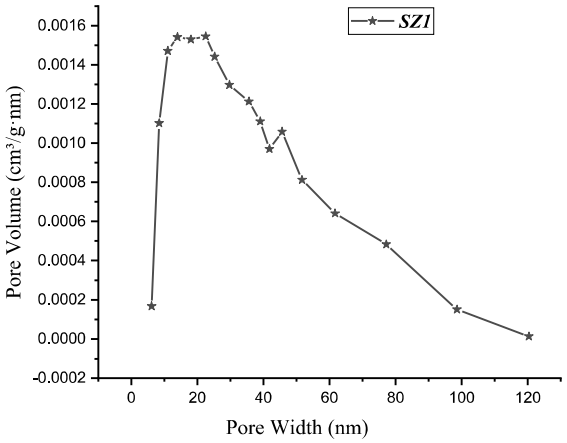
SZ1
Pore Volume (cm3/g·nm)
Pore Width (nm)

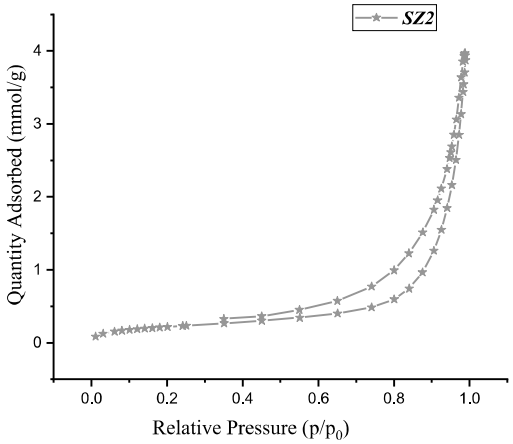
SZ2
Quantity Adsorbed (mmol/g)
Relative Pressure (p/p0)

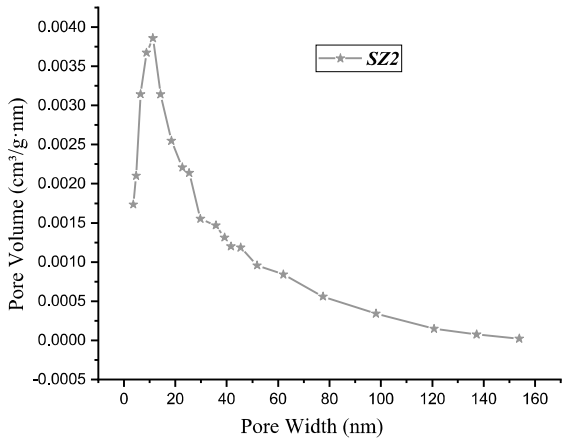
SZ2
Pore Volume (cm3/g·nm)
Pore Width (nm)

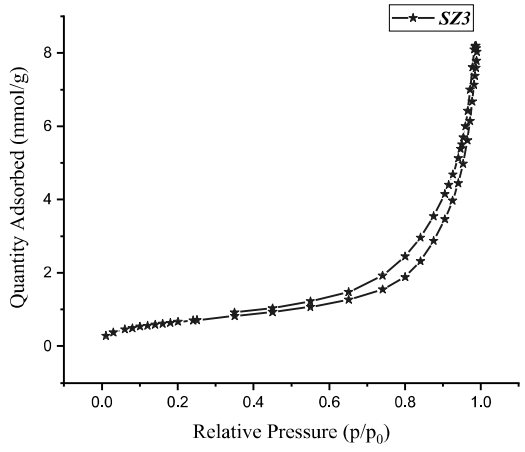
SZ3
Quantity Adsorbed (mmol/g)
Relative Pressure (p/p0)

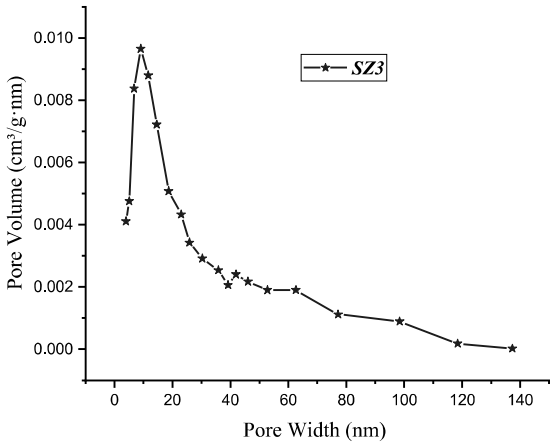
SZ3
Pore Volume (cm3/g·nm)
Pore Width (nm)

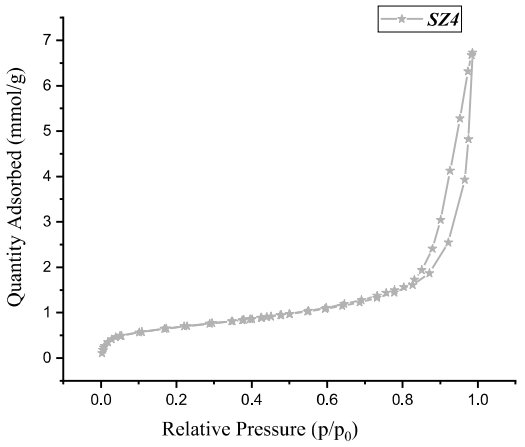
SZ4
Quantity Adsorbed (mmol/g)
Relative Pressure (p/p0)

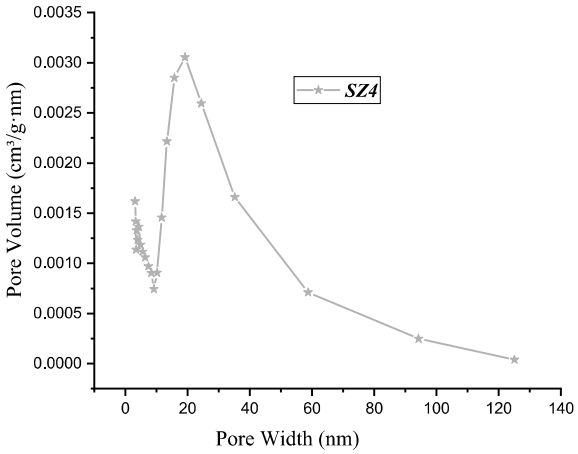
SZ4
Pore Volume (cm3/g·nm)
Pore Width (nm)

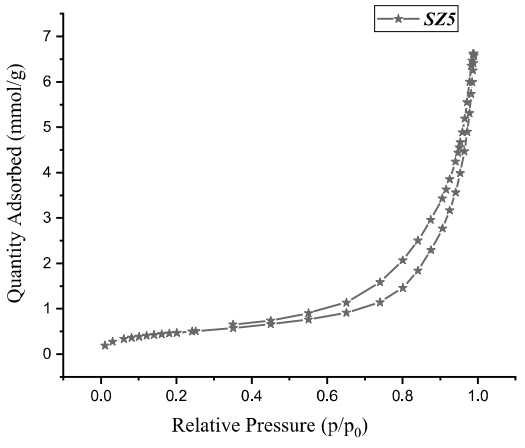
SZ5
Quantity Adsorbed (mmol/g)
Relative Pressure (p/p0)

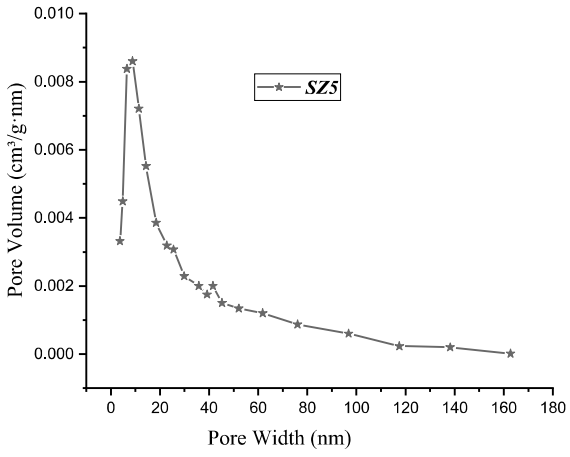
SZ5
Pore Volume (cm3/g·nm)
Pore Width (nm)

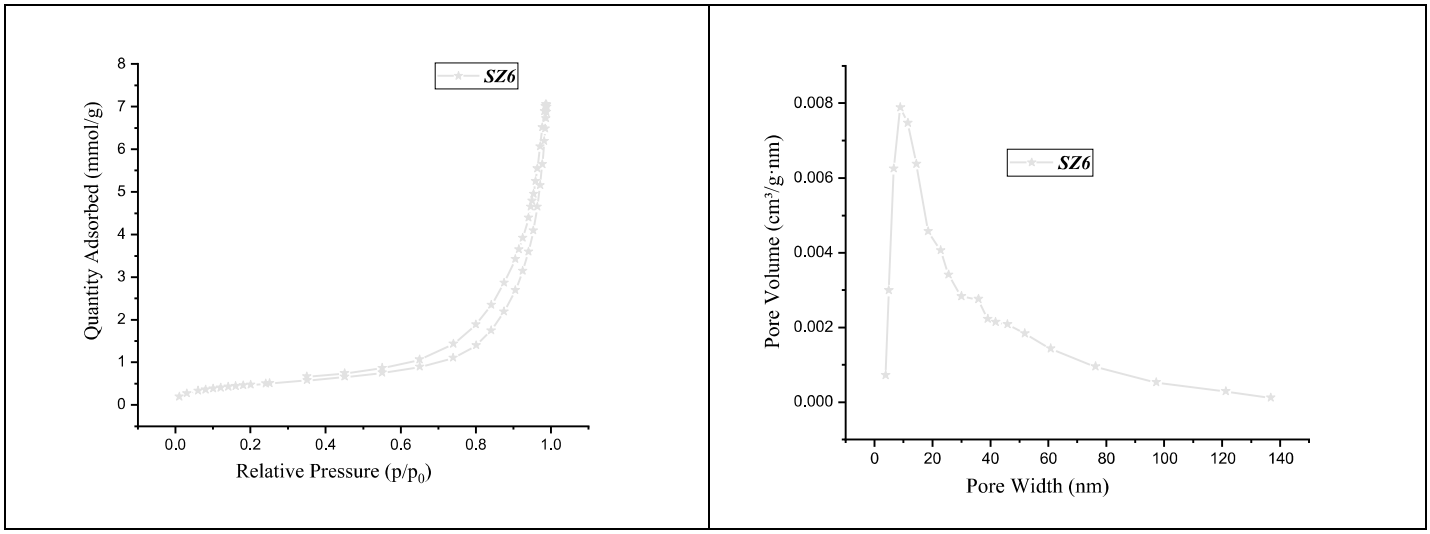

Fig. 8. Nitrogen adsorption/desorption models (a) and pore size distribution (b) of the Pristine HNC and the grafted HNC samples in several dispersing media.

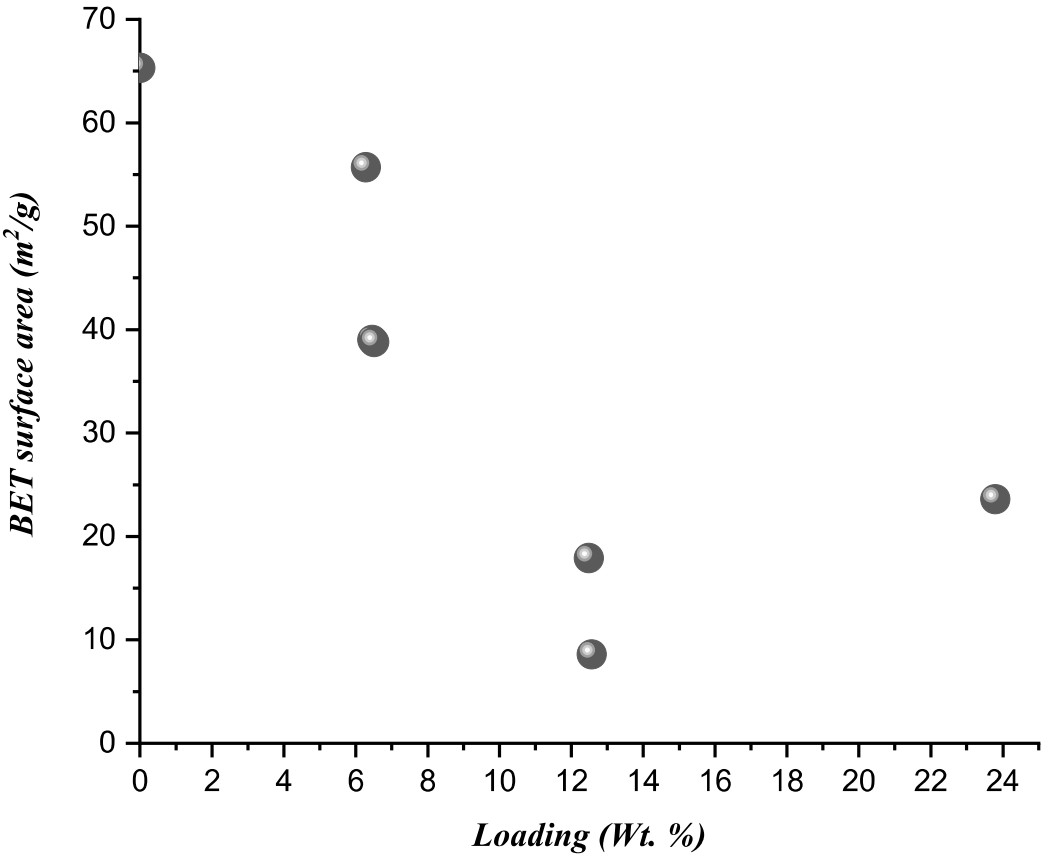

Fig. 9. Correlation between BET surface area and loading wt.%.